

# CHALMERS



## Verification of Vehicle Dynamics Control Functions

*Master's thesis in Automotive Engineering*

ERIK HARTELIUS

OSKAR EKLUND

Department of Applied Mechanics  
*Division of Vehicle Engineering and Autonomous Systems*  
*Group of Vehicle Dynamics*  
CHALMERS UNIVERSITY OF TECHNOLOGY  
Göteborg, Sweden 2014  
Master's thesis 2014:54



MASTER'S THESIS IN AUTOMOTIVE ENGINEERING

## Verification of Vehicle Dynamics Control Functions

ERIK HARTELIUS  
OSKAR EKLUND

Department of Applied Mechanics  
*Division of Vehicle Engineering and Autonomous Systems*  
*Group of Vehicle Dynamics*  
CHALMERS UNIVERSITY OF TECHNOLOGY  
Göteborg, Sweden 2014

Verification of Vehicle Dynamics Control Functions  
ERIK HARTELIUS  
OSKAR EKLUND

© ERIK HARTELIUS, OSKAR EKLUND, 2014

Master's thesis 2014:54  
ISSN 1652-8557  
Department of Applied Mechanics  
Division of Vehicle Engineering and Autonomous Systems  
Group of Vehicle Dynamics  
Chalmers University of Technology  
SE-412 96 Göteborg  
Sweden  
Telephone: +46 (0)31-772 1000

Cover:  
SAAB 9-5, Øyvind Lund

Chalmers Reproservice  
Göteborg, Sweden 2014

Verification of Vehicle Dynamics Control Functions  
Master's thesis in Automotive Engineering  
ERIK HARTELIUS  
OSKAR EKLUND  
Department of Applied Mechanics  
Division of Vehicle Engineering and Autonomous Systems  
Group of Vehicle Dynamics  
Chalmers University of Technology

## ABSTRACT

This thesis presents the development of a Model-in-the-Loop test bench which's function is to ensure system safety by verifying vehicle dynamics control functions; making sure that they do not cause any dangerous situations for a certain vehicle (e.g. SAAB 9-3) including all vehicle variants (e.g. station wagon/sedan), load cases, manoeuvres and road conditions, creating an infinitely large test matrix. This forces the test bench to be able to generate a statistically motivated finite sample from that test matrix using design of experiments, specifically Latin hypercube sampling. The test bench then simulates and analyses the vehicle behaviour in the different manoeuvres and road conditions and presents the results in a way which gives the user a good overview of the vehicle behaviour induced by the control function. An empirical study of how many simulations are needed for the results to converge is also presented. A use case, considering the development of a regenerative braking control function demonstrates the effectiveness and performance of the test bench.

Conclusions drawn include that the test bench is able to give good indicative results during the development process of a control function but also that the vehicle model needs further evaluation and verification in order for the results to be interpretable as more absolute and real. This to make them usable in the verification of a specific control function with a higher level of maturity. The vehicle model should, however, be kept fast enough to make it reasonable to run thousands of simulations as part of a development process.

Keywords: System safety, Functional safety, Vehicle dynamics modelling, Model-in-the-Loop, Design of experiments, Regenerative braking



## PREFACE

This thesis work has been conducted as a partial requirement for the Master of Science degree in Automotive Engineering at Chalmers University of Technology, Gothenburg, Sweden in cooperation with LeanNova Engineering AB, Trollhättan. The project was conducted between January and June of 2014 and the time was divided equally between Chalmers and LeanNova.

## ACKNOWLEDGEMENTS

We would like to direct a special thank you to Gunnar Olsson for his indispensable advise and mentorship throughout the whole thesis and the anecdotes that made the lunch brakes so much more enjoyable. We thank Mathias Lidberg for his effort in keeping the thesis always on the right track and providing valuable input when it was needed, Magnus Eklund for his expertise regarding all things brake related and Rudolf Brziak for the numerous, and not at all time consuming, discussions regarding everything else. To all of the employees at LeanNova Engineering AB who made us feel welcome and part of something bigger than a master's thesis, thank you. Also, thank you to Øyvind Lund for the fantastic cover art.



## NOMENCLATURE

### Symbols

$a$	= Acceleration $\frac{\text{m}}{\text{s}^2}$
$B$	= Magic Tire Formula stiffness factor
$c$	= Magic Tire Formula stiffness factor
$c_\phi$	= Roll stiffness $\frac{\text{N}}{\text{rad}}$
$C$	= Magic Tire Formula shape factor
$C_{F_\alpha}$	= Cornering stiffness $\frac{\text{F}}{\text{rad}}$
$D$	= Magic Tire Formula peak factor
$E$	= Magic Tire Formula curvature factor
$g$	= Gravitational constant $\frac{\text{m}}{\text{s}^2}$
$h$	= Roll centre height m
$I$	= Rotational inertia $\text{kgm}^2$
$k_\phi$	= Roll damping $\frac{\text{N}}{\text{rad/s}}$
$K_u$	= Understeer gradient
$l$	= Distance from CoG to wheel axle m
$L$	= Wheelbase m
$m$	= Vehicle total mass kg
$M_b$	= Braking moment Nm
$r$	= Yaw rate $\frac{\text{rad}}{\text{s}}$
$R$	= Wheel radius m
$u$	= Vehicle CoG longitudinal speed $\frac{\text{m}}{\text{s}}$
$v$	= Vehicle CoG lateral speed $\frac{\text{m}}{\text{s}}$
$w$	= Track width m
$\mathbf{x}$	= Vehicle states
$\alpha$	= Tyre lateral slip angle rad
$\beta$	= Side slip angle rad
$\gamma$	= Throttle pedal angle rad
$\delta$	= Tyre steer angle rad
$\theta$	= Brake pedal angle rad
$\kappa$	= Tyre longitudinal slip ratio %
$\mu$	= Road friction coefficient
$\sigma$	= Magic Tire Formula theoretical slip
$\sigma_{eq}$	= Magic Tire Formula equivalent slip
$\Phi$	= Roll angle rad
$\Psi$	= Yaw angle rad
$\Omega$	= Wheel rotational speed $\frac{\text{rad}}{\text{s}}$

## Sub- and superscripts

0	= At CoG or reference
1	= Axle or wheel number [Front axle / Front left tyre]
2	= Axle or wheel number [Rear axle / Front right tyre]
3	= Wheel number [Rear left tyre]
4	= Wheel number [Rear right tyre]
<i>f</i>	= Front tyres
<i>r</i>	= Rear tyres
<i>s</i>	= Sprung portion
<i>x</i>	= Longitudinal Direction
<i>xx</i>	= Around x-axis (Roll Direction)
<i>y</i>	= Lateral Direction
<i>yy</i>	= Around y-axis (Pitch Direction)
<i>z</i>	= Vertical Direction
<i>zz</i>	= Around z-axis (Yaw Direction)
$\lambda$	= Front to rear ratio

## Abbreviations

ABS	= Anti-lock Brake System
CAE	= Computer Aided Engineering
CoG	= Centre of Gravity
DIL	= Driver-in-the-Loop
DoE	= Design of Experiments
ECU	= Electronic Control Unit
ESC	= Electronic Stability Control
GUI	= Graphical User Interface
HIL	= Hardware-in-the-Loop
LHS	= Latin Hypercube Sampling
MIL	= Model-in-the-Loop
SAAB	= Svenska Aeroplan Aktie-Bolaget
SIL	= Software-in-the-Loop

# CONTENTS

<b>Abstract</b>	<b>i</b>
<b>Preface</b>	<b>iii</b>
<b>Acknowledgements</b>	<b>iii</b>
<b>Nomenclature</b>	<b>v</b>
<b>Contents</b>	<b>vii</b>
<b>1 Introduction</b>	<b>1</b>
1.1 System- and Functional Safety . . . . .	1
1.2 Verification Methods . . . . .	1
1.3 Objective . . . . .	2
1.4 Deliverables . . . . .	2
1.5 Delimitations . . . . .	2
<b>2 Model-in-the-Loop Architecture</b>	<b>3</b>
<b>3 Vehicle Model</b>	<b>5</b>
3.1 Free Body Diagrams and Equations . . . . .	5
3.1.1 Tyre Modelling . . . . .	10
3.2 Implementation . . . . .	12
3.2.1 Support Functions . . . . .	13
3.3 Response . . . . .	15
<b>4 Design of Experiments</b>	<b>19</b>
4.1 Statistical Sampling . . . . .	19
4.1.1 Evaluation of Sampling Methods . . . . .	21
4.2 Sample Size . . . . .	22
4.2.1 Convergence of Results . . . . .	22
<b>5 Use Case: Regenerative Braking</b>	<b>25</b>
5.1 Regenerative Braking . . . . .	25
5.1.1 Three Strategy Concepts . . . . .	25
5.2 Test Matrix . . . . .	26
5.2.1 Specification of Parameters . . . . .	26
5.2.2 Creation of Test Matrix . . . . .	26
5.3 Manoeuvres . . . . .	27
5.4 Criteria . . . . .	27
5.5 Initialization of Simulation . . . . .	29
5.6 Evaluation . . . . .	29
5.7 Results Generation . . . . .	30
5.8 Improvement and Iteration . . . . .	33
5.9 Final Strategy . . . . .	34
<b>6 Conclusions</b>	<b>35</b>
<b>References</b>	<b>36</b>
<b>Appendices</b>	<b>37</b>
<b>A Vehicle Initial Parameters</b>	<b>38</b>
<b>B Sampling Methods</b>	<b>39</b>

C Definition of Criteria	40
D Samples Needed for Convergence	41

# 1 Introduction

This chapter gives a background to the thesis project which declares its purpose, aims and the issues at hand. It will also put the objective and deliverables into context in a vehicle dynamics control function development process. Furthermore, the actual objective and deliverables are presented and explained.

## 1.1 System- and Functional Safety

An important but very time consuming task in vehicle development is to ensure system safety. For vehicle control functions a safe and predictable behaviour of the vehicle is required in all driving situations, i.e. the vehicle should respond as intended by the driver. This should be true for all vehicle variants, load cases, manoeuvres and all road conditions which the vehicle may operate at resulting in infinitely large test matrices in the verification phase when developing control functions. Naturally, it is impossible to physically build all these vehicle configurations and perform track testing in all these scenarios. Computer Aided Engineering (CAE) simulations are a widely used way to verify functional safety which reduces the physical testing needed, and thereby reduces the funds and time required to develop vehicles. It also makes the development process more sustainable in an environmental aspect since it limits the required production and testing of prototype vehicles. Even though CAE-simulations are relatively fast and cheap, it is still impossible to test all the scenarios mentioned above. A method for choosing how many and which simulations to execute in order to be sufficiently confident that the functions are safe and predictable needs to be developed. The term sufficiently confident itself also needs to be defined.

Functional safety is often defined as being the part of overall system safety that depends on the system taking correct actions in regards to its inputs. For the purpose of this thesis however, functional safety will rather be defined as whether the action taken is correct or not in regards to vehicle stability; whether it affects the dynamics of the vehicle in such a way that it causes hazardous situations.

## 1.2 Verification Methods

Depending on in which stage of the development process a control function is different CAE methods are used to verify its quality and functional safety. These methods include, but are not limited to, simulations run with model-in-the-loop (MIL), software-in-the-loop (SIL), hardware-in-the-loop (HIL) and driver-in-the-loop (DIL). MIL simulations are run when the control function is still in its concept stage in the form of a simple algorithm. The function is simulated with inputs and outputs (I/O) to a simulated environment, represented by a model in e.g. Simulink. When doing SIL testing the control model has reached a higher level of maturity and is properly coded in a computer program, implementable in an ECU. The function is now simulated with time discrete I/O to a simulated environment. HIL takes it even further as the software gets implemented in one or more ECUs and is tested in real-time with I/O to a simulation model. The control functions can also be evaluated in a DIL environment, where the driver is part of the loop, e.g. a driving simulator.

Development is fastest during MIL simulations but only issues induced by the strategical algorithm itself are discovered at this stage. SIL testing is required to detect software errors and bugs in the code. Further, HIL testing is needed to capture electrical and hardware errors. DIL simulations are not as widely used as the previously described three types. However, feedback from an actual driver can prove to be useful, since the feel of the vehicle is a vague and diffuse term, sometimes hard to quantify and evaluate in CAE simulations. These methods can also be used to analyse how the function responds to failure modes such as signal losses and errors by introducing them purposely to the simulation.

## 1.3 Objective

The objective of the thesis is to create a model-in-the-loop test bench that is able to, for a given control function, verify safe and predictable behaviour from a vehicle dynamics perspective, on a model level. To be able to do this efficiently, a design of experiments (DOE) method needs to be chosen, evaluated and developed so that it reduces the number of samples to an amount where the time it takes to simulate the test matrix is reasonable in the early stages of a development process. Also, an investigation into how many samples that are sufficient for the results to converge needs to be conducted. In order to allow for evaluation/demonstration of the effectiveness of the test bench, a use case will be presented.

## 1.4 Deliverables

The following items are to be delivered by the end of the thesis project:

### Model-in-the-Loop Test Bench

- Simulation environment
- Design of experiments
  - Sampling method
  - Population size
  - Study of convergence
- Evaluation of vehicle behaviour
- Results generation
- Graphical User Interface (GUI)
- Batch processing

### Use Case

- Control function
- Specification of parameters to vary
- Manoeuvres
- Environmental conditions
- Criteria

The architecture of the Model-in-the-Loop test bench, as well as a definition of the above declared items will be given in Chapter 2.

## 1.5 Delimitations

The vehicle considered in the thesis will be limited to one based on a SAAB 9-3, since it is available beforehand. The simulation environment will be limited to MIL-simulations and will primarily be able to handle the control function in its model stage. Also, the vehicle model used will not be verified against a physical vehicle.

## 2 Model-in-the-Loop Architecture

As the objective of the thesis states, the purpose of the developed tool is to verify safe and predictable vehicle behaviour for a given control function. The method used to achieve this via the Model-in-the-Loop test bench developed in this project will be described in this chapter, as well as the architecture and flow of information within the test bench. Further, a brief description of the containing blocks will be given.

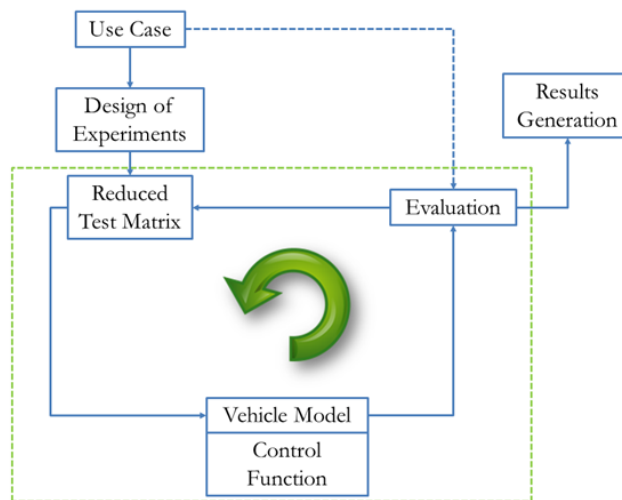


Figure 2.1: *Model-in-the-Loop test bench architecture*

Figure 2.1 illustrates the general structure of the MIL test bench as well as gives overview of the flow of information. Following is a description of the containing blocks in chronological order of usage:

### Use Case

In order to set up the verification process of a control function, a use case must be defined. The use case block contains all the inputs required by the Model-in-the-Loop test bench to start the process. A demonstration of a use case is exhibited in Chapter 5. The four types of information required to set up the process are:

- **Vehicle Parameters:**  
A chosen number of vehicle parameters, with corresponding limits under which the control function could operate within. Examples are vehicle total mass 1500-2000kg, weight distribution 40-48% and center of gravity height 0.5-0.8m. This is to verify that the control function is safe and predictable in any possible vehicle configuration and loading.
- **Manoeuvres:**  
A number of specified critical manoeuvres to be used for evaluating the control function, e.g. braking in turn, single lane change and straight line braking.
- **Environmental conditions:**  
Events of environmental influence such as dry asphalt, ice or split- $\mu$ .
- **Criteria:**  
Collection of manoeuvre dependent criteria which are used for evaluating the performance of the vehicle simulations. The criteria are used in the Evaluation block and consists of maximum or minimum allowed limits on parameters such as longitudinal- and lateral acceleration or yaw rate.

## **Design of Experiments**

The infinite amount of vehicle combinations from the Use Case block are reduced to a finite amount in the Reduced Test Matrix. The method for determining the population size of this Reduced Test Matrix is in detail explained in Chapter 4. The method for efficiently generating points in this population is also explained and demonstrated in the same chapter. The generated points are hereinafter referred to as samples.

## **Vehicle Model**

One of the samples are sent to the Vehicle Model block, where the vehicle dynamics calculations are executed. The sample is simulated performing the manoeuvres specified in the Use Case block under the environmental conditions also specified there. The Vehicle Model block is also where the specified control function is modelled. The vehicle model is explained in detail in Chapter 3.

## **Evaluation and Results Generation**

The simulation results are saved and sent to the Evaluation block, where they are compared to the criteria as specified in the Use Case block. In the evaluation process, the software assigns an attribute to each sample which is either pass or fail, for every criteria. This information is stored in the Results Generation block. The way the results are displayed is shown in Chapter 5.

## **Loop**

When the current simulation is evaluated, the test bench picks the next sample from the predefined Reduced Test Matrix and sends this sample to the Vehicle Model, where it is simulated and evaluated as earlier described. This process is repeated until every sample in the Reduced Test Matrix is simulated for the specified manoeuvres and environmental conditions. The results are compiled into a results report where the user gets an overview of the results.

## **Graphical User Interface**

The user will interact with the MIL test bench via a graphical user interface (GUI) as demonstrated in Chapter 5. To set up the test bench, the user inputs entries as listed in the description of the Use Case block. When the loop is completed and the results report is generated, the user has the ability to study the simulations in detail via the GUI. Examples are scatter plots for vehicle parameters and criteria, such as studying how the weight distribution affects the yaw rate, single simulation plots (e.g. tyre forces, wheel speeds, vehicle accelerations) and vehicle trajectory plots.

At this point, the user has developed an understanding of how the specified vehicle dynamics control function performs with different vehicle parameters and under different manoeuvres and environmental conditions and can, depending on the results, either make proper adjustments to the control function or proceed to the next stage in the development process.

### 3 Vehicle Model

This chapter describes the vehicle model of the MIL test bench and presents the equations used to simulate the vehicle behaviour. The model is based on a model developed as part of an assignment in the course *TME102 Vehicle Dynamics, Advanced* given at Chalmers University of Technology, Gothenburg and is chosen and modified to be time efficient while still capturing the effects of importance caused by the specific control function described in Chapter 5. The model part of the MIL test bench is a detachable block and can be replaced by a different vehicle model, depending on the requirements for verifying a different control function than the one described in Chapter 5.

The vehicle model is a two track model with a coordinate system according to ISO 8855 [4]. The model is valid for front wheel steered passenger car with two wheel axles. Combined tyre slip and tyre forces are calculated according to *Tyre and Vehicle Dynamics* [7]. The model includes four rotating wheels with individual wheel speeds. The friction coefficient is modelled to decrease with increased vertical load and tyre relaxation has been taken into account. Load transfer is modelled dynamically in roll direction and for steady state accelerations in pitch. The brake system is modelled to generate a wheel braking moment linearly proportional to the brake pedal angle.

Effects and systems which are not included due to their relatively small respective influence in this specific case are rolling resistance, a drive train, aerodynamics and suspension geometry influences. Further, the model does not include an ESC (Electronic Stability Control) system or a driver model.

#### 3.1 Free Body Diagrams and Equations

This section presents the coordinate system, free body diagrams and equations used in the simulation environment.

##### Coordinate System

The coordinate system used is defined by the standard ISO 8855 and is shown in Figure 3.1, with positive  $x$  being forwards,  $y$  to the left and  $z$  upwards.

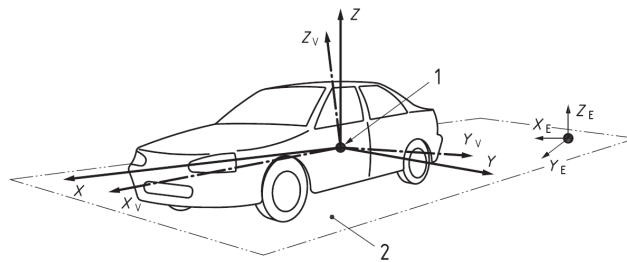


Figure 3.1: ISO 8855 vehicle coordinate system

The pitch, roll and yaw directions of rotation are also set according to ISO 8855 with positive yaw being the angle from  $X_E$  to  $X$  around  $Z_E$ , pitch the angle from  $X$  to  $X_V$  around  $Y$ , and roll the angle from  $Y$  to  $Y_V$  around  $X_V$ .

The free body diagram with corresponding notations is shown in Figure 3.2. The vehicle is front wheel steered only and without Ackermann steering geometry, which leads to  $\delta_1 = \delta_2 = \delta_f$  and  $\delta_3 = \delta_4 = 0$

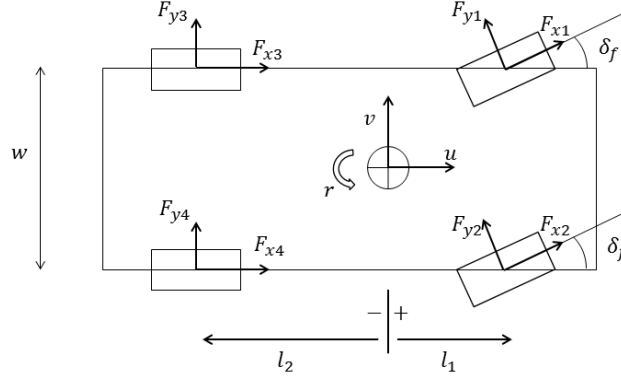


Figure 3.2: Free body diagram

### Equations of Motion

The equations of motion in longitudinal, lateral and yaw direction are based on the Newton second laws of motion, i.e.  $ma = \sum F$ , and  $J\dot{\omega} = \sum M$ . Due to the steering angle of the wheels, the wheel forces need to be divided into longitudinal and lateral components in the vehicle coordinate system. These fractions are given by:

$$\mathbf{F}_{long} = \mathbf{F}_x \cos \delta - \mathbf{F}_y \sin \delta \quad (3.1)$$

$$\mathbf{F}_{lat} = \mathbf{F}_y \cos \delta - \mathbf{F}_x \sin \delta \quad (3.2)$$

In order to be able to perform calculations in vector form for the four wheels, we add the identity vector as:

$$\mathbf{I}_4 = \begin{bmatrix} 1 \\ 1 \\ 1 \\ 1 \end{bmatrix} \quad (3.3)$$

The centripetal acceleration gives that  $a_x = \dot{u} - vr$  and  $a_y = \dot{v} + ur$ . This together with the Newton second laws of motion and the distances from centre of gravity to the wheels,  $\mathbf{w}$  and  $\mathbf{l}$ , gives the time derivative of the vehicle longitudinal and lateral speeds,  $u$  and  $v$ , as well as the yaw rate  $r$  as:

$$\dot{u} = \frac{\mathbf{I}'_4 \cdot \mathbf{F}_{long}}{m} + vr \quad (3.4)$$

$$\dot{v} = \frac{\mathbf{I}'_4 \cdot \mathbf{F}_{lat}}{m} - ur \quad (3.5)$$

$$\dot{r} = \frac{\mathbf{w}' \cdot \mathbf{F}_{long} + \mathbf{l}' \cdot \mathbf{F}_{lat}}{I_{zz}} \quad (3.6)$$

## Lateral Slip Angles

The lateral slip angles are defined according to ISO 8855 as shown in Figure 3.3. The compatibility equation for steering-, lateral slip- and side slip angles is obtained as:

$$\beta = \delta - \alpha \quad (3.7)$$

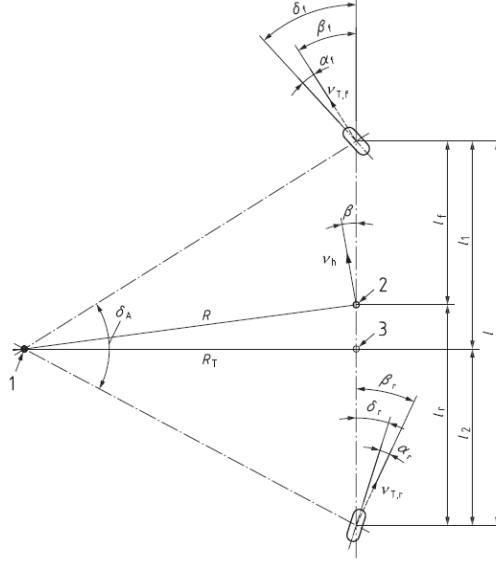


Figure 3.3: ISO 8855 lateral slip angles

The side slip angle  $\beta_i$  for every wheel is given by the arctangent of the fraction between the wheel lateral and longitudinal speed (with wheel indexes according to Figure 3.2).

$$\beta_i = \arctan \frac{v_{yw_i}}{v_{xw_i}} \quad (3.8)$$

The wheel lateral and longitudinal speeds are given by the vehicle speed and the yaw rate times the distance to the wheel as:

$$v_{xw} = u + \omega \cdot r \quad (3.9)$$

$$v_{yw} = v + l \cdot r \quad (3.10)$$

The above mentioned distances are given by the track width  $w$  and the distances from center of gravity to the wheel axles  $l_1$  and  $l_2$  (with  $l_2$  being a negative distance according to Figure 3.2):

$$l = \begin{bmatrix} l_1 \\ l_1 \\ l_2 \\ l_2 \end{bmatrix} \quad (3.11)$$

$$w = \frac{1}{2} \begin{bmatrix} -w \\ w \\ -w \\ w \end{bmatrix} \quad (3.12)$$

The tyre lateral slip angle for every wheel  $\alpha_i$  can now be calculated as:

$$\alpha_i = \delta_i - \arctan \frac{v_{yw_i}}{v_{xw_i}} \quad (3.13)$$

### Longitudinal Slip Ratio

The longitudinal tyre slip  $\kappa_i$  is for every wheel defined as the following ratio, with the minus-sign added so that a positive  $\kappa$  generates a positive force  $F_x$ .

$$\kappa_i = -\frac{\Omega_{0_i} - \Omega_i}{\Omega_{0_i}} = -\left(1 - \frac{\Omega_i}{\Omega_{0_i}}\right) \quad (3.14)$$

Here  $\Omega_0$  are the reference wheel rotational speeds, i.e. the speeds which the wheels would rotate with in the case of 0 slip.  $\Omega$  are the actual wheel rotational speeds. The reference wheel speeds can be obtained by dividing the wheel longitudinal speed with its radius:

$$\Omega_0 = \frac{v_{xw}}{R} \quad (3.15)$$

To find the actual wheel speeds  $\Omega$ , Newtons 2nd law for rotating systems gives the following equation where  $M_b$  is the braking or acceleration moment on the wheel,  $R$  the wheel radius and  $I_{w_{yy}}$  the wheel rotational inertia:

$$\dot{\Omega} = \frac{M_b - F_x R}{I_{w_{yy}}} \quad (3.16)$$

The actual wheel speeds  $\Omega$  are found by numerically integrating  $\dot{\Omega}$  in the equation above.

## Load Transfer

The vertical load on the wheels at a given time is the static weight plus the change in load in longitudinal and lateral direction.

$$\mathbf{F}_z = \mathbf{F}_{zStatic} + d\mathbf{F}_{zx} + d\mathbf{F}_{zy} \quad (3.17)$$

The steady state load transfer in longitudinal direction when braking or accelerating is given by Equation 3.18, generated by balancing forces during longitudinal acceleration. When accelerating (positive  $a_x$ ), load increases on rear tyres and when braking (negative  $a_x$ ), load increases on front tyres.

$$d\mathbf{F}_{zx} = \begin{bmatrix} -1 \\ -1 \\ 1 \\ 1 \end{bmatrix} \cdot \frac{mha_x}{2L} \quad (3.18)$$

The dynamic load transfer in lateral direction is obtained by balancing the forces on the front and rear axle separately. The two cases is combined into one expression in Equation 3.19 . Positive lateral acceleration (to the left) gives increase in load on right hand tyres (2 and 4) and decrease in load on left hand tyres (1 and 3) and vice versa for negative lateral acceleration.

$$d\mathbf{F}_{zy} = \begin{bmatrix} -1 \\ 1 \\ -1 \\ 1 \end{bmatrix} \cdot \frac{1}{w} \left( \frac{m(L-l)a_y \mathbf{h}}{L} + \mathbf{c}_\Phi \dot{\Phi} + \mathbf{k}_\Phi \Phi \right) \quad (3.19)$$

Here we have that  $\mathbf{l} = [l_1 \ l_1 \ -l_2 \ -l_2]^T$  which gives the distances from center of mass to the corresponding wheel axles, along the x-axis. The vector  $\mathbf{h} = [h_1 \ h_1 \ h_2 \ h_2]^T$  gives the correct roll center height at the corresponding axle.  $\mathbf{c}_\Phi$  and  $\mathbf{k}_\Phi$  are defined as  $[c_{\Phi_1} \ c_{\Phi_1} \ c_{\Phi_2} \ c_{\Phi_2}]^T$  and  $[k_{\Phi_1} \ k_{\Phi_1} \ k_{\Phi_2} \ k_{\Phi_2}]^T$  and assigns the roll-stiffness and damping to the corresponding axle.

The roll- angle  $\Phi$  and velocity  $\dot{\Phi}$  are found by numerically integrating the roll acceleration  $\ddot{\Phi}$ . By balancing moments around the vehicle roll axis and using the parallel axis theorem for determining the vehicle inertia around the roll axis, the roll acceleration is obtained as:

$$\ddot{\Phi} = \frac{m_s a_y h_0 - k_\Phi \dot{\Phi} - (c_\Phi - m_s g h_0) \Phi}{I_{xx} + m_s h_0^2} \quad (3.20)$$

where  $c_\Phi$  and  $k_\Phi$  are the vehicle total roll- stiffness and damping and  $h_0$  is the height of center of gravity above roll axis, calculated as (see [5]):

$$h_0 = h - \frac{l_1 h_2 - l_2 h_1}{L} \quad (3.21)$$

### 3.1.1 Tyre Modelling

The tyre forces are modelled according to a semi-empirical model called the Magic Tyre Formula described in *Tyre and Vehicle Dynamics* [7]. Semi-empirical models have specially been developed to function as parts of simulation environments. The name semi-empirical implies that it is not only based on observation and measurements like an empirical model, but the coefficients in the equations have a connection to physical attributes e.g. cornering stiffness and maximum force as this subsection will show. The general shape of the Magic Tyre Formula is shown in Figure 3.4.

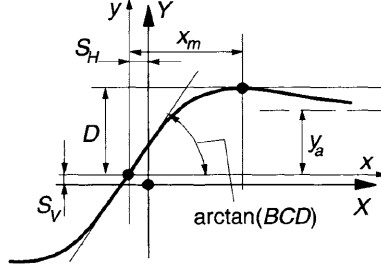


Figure 3.4: General shape of the Magic Tyre Formula

The Magic Tyre Formula can create curves which resemble curves from measured tyre data for lateral and longitudinal tyre forces. The produced curve passes through the origin, reaches a maximum value and then decreases like a real tyre. The general equation for the curve is given by:

$$y = D \sin(C \arctan(Bx - E(Bx - \arctan Bx)))) \quad (3.22)$$

where  $B$  is a stiffness factor,  $C$  a shape factor,  $D$  the peak value and  $E$  a curvature factor. The variable  $x$  is lateral or longitudinal slip and  $y$  gives the tyre force.

When a vehicle is simultaneously braking or accelerating and turning, the above mentioned formula will not give realistic results. A tyre cannot produce the maximum lateral force if the vehicle is braking or accelerating at the same time. Neither can it produce the maximum longitudinal force if the vehicle is turning at the same time. The force a tyre can generate is widely estimated as a circle, called the friction circle. Its general shape is shown in Figure 3.5. However, the physically measured shape resembles an ellipse more than a circle.

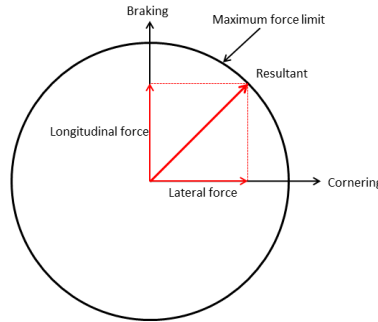


Figure 3.5: Friction circle

To take this limit into account, we introduce term  $\sigma^*$  as:

$$\sigma^* = \sqrt{\sigma_x^2 + \sigma_y^2} \quad (3.23)$$

where  $\sigma_x$  and  $\sigma_y$  are the theoretical slip angles given by (see [7] for derivation):

$$\sigma_x = \frac{\kappa}{1 + \kappa} \quad (3.24)$$

$$\sigma_y = \frac{\tan \alpha}{1 + \kappa} \quad (3.25)$$

The variable  $\sigma^*$  together with the fractions  $\frac{\sigma_x}{\sigma^*}$  and  $\frac{\sigma_y}{\sigma^*}$  will scale the tyre- slip and forces according to the friction circle limitation. In order to realistically model the tyre forces, degradation by means of increased vertical load of the friction coefficient  $\mu$  and cornering stiffness  $C_{F\alpha}$  must be accounted for. Hence, the fractions  $\frac{C_{F\alpha}}{C_{F\alpha 0}}$ ,  $\frac{\mu_x}{\mu_{x0}}$  and  $\frac{F_z}{F_{z0}}$  are introduced.

The cornering stiffness at a given vertical load on a wheel is given by:

$$C_{F\alpha} = c_1 c_2 F_{z0} * \sin \left( 2 \arctan \left( \frac{F_z}{c_2 F_{z0}} \right) \right) \quad (3.26)$$

where  $c_1$  and  $c_2$  are stiffness factors and  $F_{z0}$  is the rated load for the tyre. The cornering stiffness at static load is calculated as:

$$C_{F\alpha 0} = c_1 c_2 F_{z0} * \sin \left( 2 \arctan \left( \frac{F_{zStatic}}{c_2 F_{z0}} \right) \right) \quad (3.27)$$

The friction coefficient is modelled to decrease with vertical load according to:

$$\mu_x = \mu_{x0} (1 - \mu_1 (F_z - F_{z0})) \quad (3.28)$$

$$\mu_y = \mu_{y0} (1 - \mu_1 (F_z - F_{z0})) \quad (3.29)$$

where  $\mu_1$  is a tyre load based non-linearity parameter for friction which is given by observing tyre data.

We can now produce the equivalent tyre slip  $\sigma_{eq}^x$  and  $\sigma_{eq}^y$  in lateral and longitudinal direction respectively as:

$$\sigma_{eq}^x = \frac{C_{F\alpha}}{C_{F\alpha 0}} \frac{\mu_{x0}}{\mu_x} \frac{F_z}{F_{z0}} \sigma^* \quad (3.30)$$

$$\sigma_{eq}^y = \frac{C_{F\alpha}}{C_{F\alpha 0}} \frac{\mu_{y0}}{\mu_y} \frac{F_z}{F_{z0}} \sigma^* \quad (3.31)$$

With the equivalent slip quantities, we are able to calculate the tyre forces at nominal load according to the Magic Tyre Formula (Equation 3.22) as:

$$F_{x0} = D_{x0} \sin \left( C_x \arctan \left( B_{x0} \sigma_{eq}^x - E_x (B_{x0} \sigma_{eq}^x - \arctan (B_{x0} \sigma_{eq}^x)) \right) \right) \quad (3.32)$$

$$F_{y0} = D_{y0} \sin \left( C_y \arctan \left( B_{y0} \sigma_{eq}^y - E_y (B_{y0} \sigma_{eq}^y - \arctan (B_{y0} \sigma_{eq}^y)) \right) \right) \quad (3.33)$$

The shape factors  $C_x$  and  $C_y$  as well as the curvature factors  $E_x$  and  $E_y$  are tyre specific parameters and are obtained by tuning against tyre data. The peak factors  $D_{x0}$  and  $D_{y0}$  are given from the road friction and the nominal load as:

$$D_{x0} = \mu_{x0} F_{z0} \quad (3.34)$$

$$D_{y0} = \mu_{y0} F_{z0} \quad (3.35)$$

The stiffness factors  $B_{x0}$  and  $B_{y0}$  are obtained by the cornering stiffness, the curvature factors and the peak factors as:

$$B_{x0} = \frac{C_{F\alpha 0}}{C_x D_{x0}} \quad (3.36)$$

$$B_{y0} = \frac{C_{F\alpha 0}}{C_y D_{y0}} \quad (3.37)$$

The tyre forces in longitudinal and lateral direction can finally be computed as:

$$F_x = \frac{\sigma_x}{\sigma^*} \frac{\mu_x}{\mu_{x0}} \frac{F_z}{F_{z0}} F_{x0} \quad (3.38)$$

$$F_y = \frac{\sigma_y}{\sigma^*} \frac{\mu_y}{\mu_{y0}} \frac{F_z}{F_{z0}} F_{y0} \quad (3.39)$$

## 3.2 Implementation

The vehicle model has been implemented in the software Mathworks Simulink. The architecture of the model is shown in Figure 3.6. The model uses the equations shown in Section 3.1.

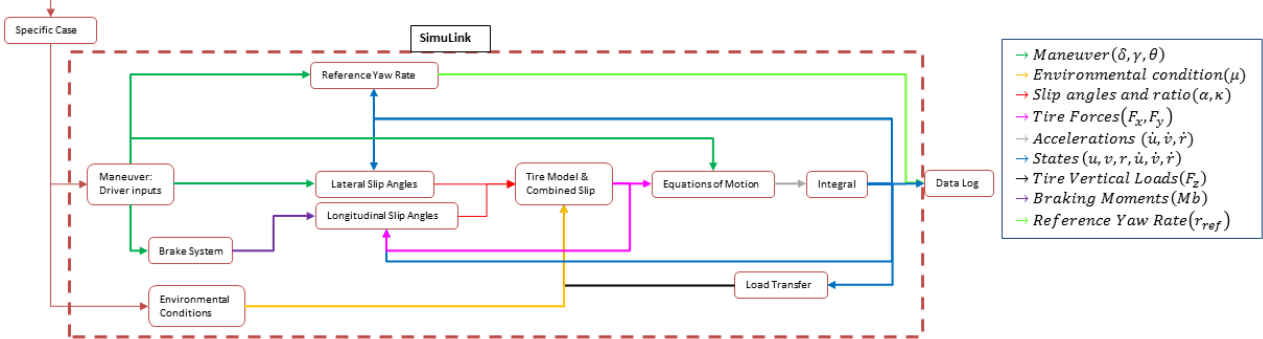


Figure 3.6: *Simulink vehicle model architecture*

Input to the model is a specific case consisting of a combination of the following parameters:

- Vehicle parameters such as mass, weight distribution and center of gravity
- Environmental conditions such as dry asphalt, ice or split- $\mu$
- A specific manoeuvre e.g. braking in turn or lane change

The specific case generates the variables steering angle  $\delta$ , throttle pedal angle  $\gamma$  and brake pedal angle  $\theta$ . These variables generate tyre slip angles and ratios through the vehicle brake- and steering system. Furthermore, the slip of the tyres generate forces acting on the vehicle, changing its states via the equations of motion.

As mentioned earlier in this chapter, the vehicle model is based on a model which was developed in a course at Chalmers University of Technology. The additions which were made to be able to capture the effects of the control function described in Chapter 5 include:

- Rotating wheels
- Brake system with hydraulic lag
- Longitudinal slip calculations
- Combined- slip and tyre force model
- Possibility for brake- and throttle pedal inputs
- Possibility to visualize both actual- and reference car trajectory
- Anti-lock braking (ABS) system
- Select-low strategy for the ABS

Equations for the rotating wheels and the tyre- slip and forces have been presented in Section 3.1 and the ABS, select-low strategy and hydraulic lag will be described in Subsection 3.2.1.

### 3.2.1 Support Functions

In order to simulate a realistic modern passenger car, the above described equations of motion is not sufficient. A vehicle today has a number of support functions that needs to be accounted for. There are also physical limitations on the response speed of tyres, hydraulics in the brake system etc. This section describes how these matters have been taken into consideration and Section 3.3 contains simulation results with the functions operating. Additionally, extra state derivatives had to be implemented to the model in order for the software to be able to solve the equations.

#### ABS

The Anti-lock Braking System (ABS) keeps the wheels from locking and helps to increase the braking capability as well as maintaining steering ability under hard braking. It is modelled to check the longitudinal slip according to Equation 3.14 for every wheel with a constant frequency, independently of the simulation sampling frequency. This it to simulate that the vehicle has wheel speed sensors measuring speed with a frequency different from the simulation step size, and it is implemented with a rate transition function. The modelled ABS system compares the longitudinal tyre slip individually for each tyre to a specified maximum allowed tyre slip. If the longitudinal tyre slip is over a specified maximum limit, the system drops the brake pressure to this individual wheel.

#### Select Low

Modern ABS systems often use the 'select low' strategy on the rear axle of the vehicle. The function is to distribute the same brake pressure to both of the rear wheel brakes. The pressure is determined by the wheel that has the greatest tendency to lock. This strategy helps retaining cornering ability of the rear tyres especially while driving on split- $\mu$ . The function is generally not used on the front axle, since it would drastically decrease the braking capability of the vehicle. The strategy is modelled to compare the magnitude of the braking moments that the ABS distributes, via the brake pressure, to the rear wheels and apply the lowest of the two to both wheels.

#### Reference Yaw Rate

The reference yaw rate is added to the model for evaluation purposes. It is not used for any active system in the vehicle model. The user has the possibility to set limits on criteria related to the reference yaw rate in order to capture simulations where the vehicle is under- or over steering.

The front and rear axle cornering stiffness, as well as the understeer gradient need to be calculated in order to obtain the reference yaw rate. The axle cornering stiffnesses are given by adding the tyre stiffness  $C_{F\alpha 0}$ , calculated with Equation 3.27, for the two wheels for each axle. Axle stiffness is noted as  $C_{F_{axle}}$ . The understeer gradient is calculated as Equation 3.40 and the reference yaw rate is obtained by Equation 3.41 (remember that  $l_2$  is defined as negative according to Figure 3.2).

$$K_u = \frac{m}{L} \left( \frac{l_2}{C_{F_{axle1}}} + \frac{l_1}{C_{F_{axle2}}} \right) \quad (3.40)$$

$$r_{ref} = \frac{\delta_f u}{L + K_u \frac{u^2}{g}} \quad (3.41)$$

## Tyre Relaxation

When a slip angle is introduced to a tyre there is a delay before the force is built up to a steady state value. This phenomena is called tyre relaxation and is accounted for in the vehicle model. The delay is specified as a distance  $L_r$ , the relaxation length, i.e. the rolling distance it takes to build up to a steady state tyre force. The rate of change in the force generated by the tyre is modelled as:

$$\dot{F} = \frac{F_{theoretical} - F}{L_r/u} \quad (3.42)$$

where  $u$  is the longitudinal velocity of the vehicle and  $L_r/u$  is the time it takes for the tyre to roll the relaxation length. By taking the Laplace transform of Equation 3.42 and dividing  $F_{theoretical}$  with  $F$ , the transfer function between the theoretical force and the force generated with tyre relaxation taken into account becomes as Equation 3.43. This transfer function is implemented for each tyre in the vehicle model to simulate the tyre relaxation.

$$H_{TR} = \frac{1}{\frac{L_r}{u}s + 1} \quad (3.43)$$

## Hydraulic Lag

Like the tyre force described above, the hydraulic system also has limitations in response time. In case the ABS system commands maximum or zero brake pressure, the actual brake pressure would not reach those levels instantly. This hydraulic lag is modelled with a simple transfer function shown in Equation 3.44 with describes the relation between the commanded- and actual brake pressure. The coefficient  $h_l$  sets the maximum rate of change in actual brake pressure and is obtained by physical measurements of response time in the brake system.

$$H_{HL} = \frac{1}{h_l s + 1} \quad (3.44)$$

### 3.3 Response

The original model used in the course mentioned in the beginning of the chapter was used with a sampling frequency of 50 Hz with sufficient results. When introducing rotating wheels and longitudinal slip calculations the simulations showed unstable and oscillatory behaviour as seen in Figure 3.7. The graphs are produced during a straight line braking manoeuvre with the labels FL, FR, RL and RR corresponding to the individual tyres with the first letter being Front/Rear and the second being Left/Right.

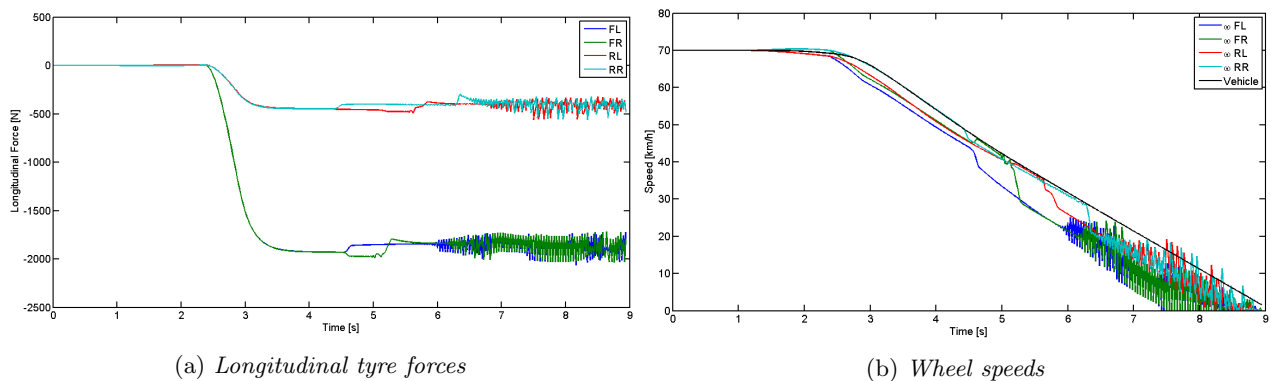


Figure 3.7: Simulation response at 50 Hz

The sampling frequency required an increase to 1000 Hz before the response was stable and realistic. The response at 1000 Hz is shown in Figure 3.8.

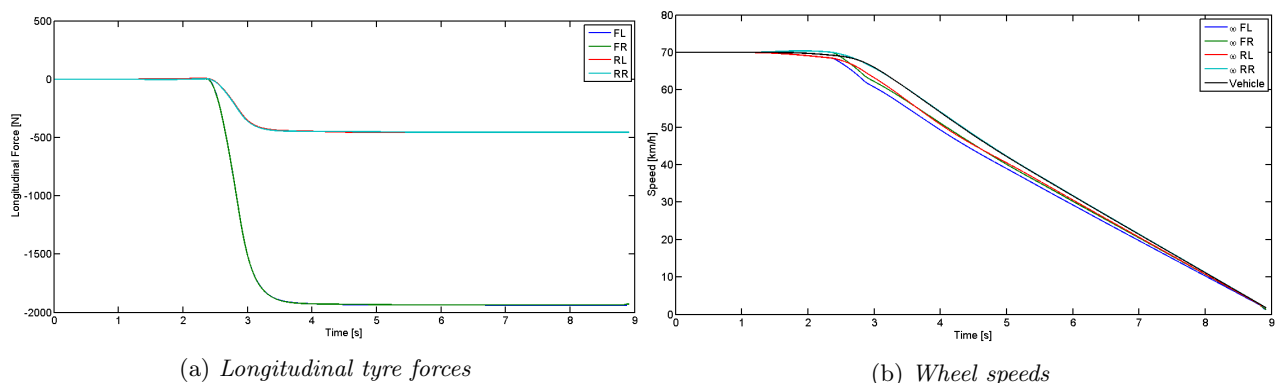


Figure 3.8: Simulation response at 1000 Hz

This change of sampling frequency increased the simulations times from 1.6 seconds for one manoeuvre on a standard lap-top, to 5.5 seconds. The MIL test bench is built to run large amount of simulations and it needs to be time efficient in order to be useful in a development process, hence this increase in simulation time is unacceptable. The option of running simulations with variable step size was disregarded since the actual time step is needed to calculate extra state derivatives, used to avoid an algebraic loop.

The model developed at Chalmers was implemented using only embedded Matlab blocks in Simulink, which was found to be very disadvantageous for running multiple simulations. The reason is that when an Interpreted Matlab function block is included in the model, the Matlab interpreter is called at each time step during the simulation. This drastically slows down the simulation time [6]. Instead, the model developed in this project was chosen to be implemented using only Simulink blocks to execute the calculations. The simulation time was empirically tested and found to be reduced from 5.5 seconds to roughly 0.8 seconds, reducing the time required by a factor of almost 7. Simulations were shown to require less time at 1000 Hz using only Simulink blocks, than 50 Hz using Interpreted Matlab functions. However, for executing low amounts of simulations, the textual

language of the Matlab function blocks makes it simpler for the user to write functions and algorithms and gives a better overview of the code. In the case of running large scale quantities of Simulink simulations, the user is strongly advised to avoid Matlab function blocks in the model. The graphical language of Simulink was shown to be more complicated for implementing functions and algorithms, especially conditional statements, e.g. if- and switch expressions.

Running the vehicle model using only Simulink blocks at 1000 Hz gives stable and realistic results. Following are examples of plots extracted from the vehicle model running at these conditions. The vehicle parameters are as listed in Appendix A. The vehicle model has not been compared or validated to other vehicle models or physical testing data.

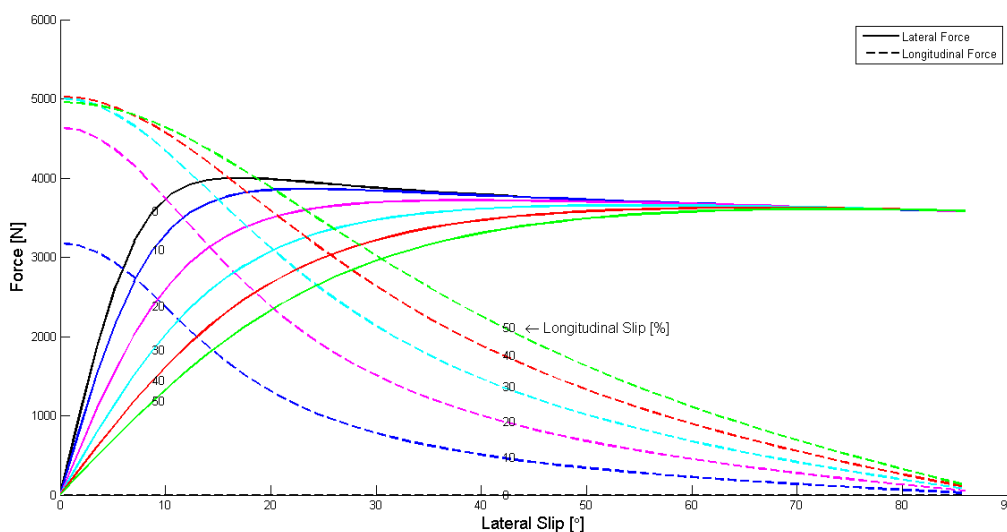


Figure 3.9: *Tyre forces vs lateral slip*

Figure 3.9 illustrates how the tyre forces vary with lateral slip in the case of combined slip. The plot is produced at static vertical load for six different longitudinal slip ratios  $\kappa$ : 0%(black), 10%(blue), 20%(pink), 30%(cyan), 40%(red) and 50%(green). The curves starting from the origin represent the lateral forces (since  $F_y = 0$  when  $\alpha = 0$ ) and the others represent the longitudinal forces. It is clear that the longitudinal slip  $\kappa$  heavily affects the available lateral force. The figure also shows that the lateral slip  $\alpha$  has the same effect on the available longitudinal force. The curve for  $\kappa = 0\%$ (black) is not visible in the graph since no longitudinal force will be generated under this condition.

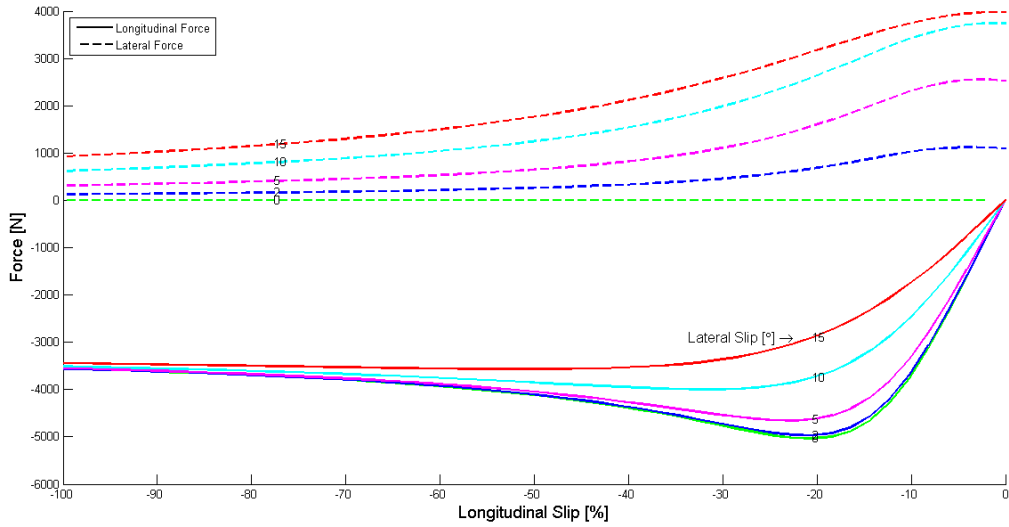
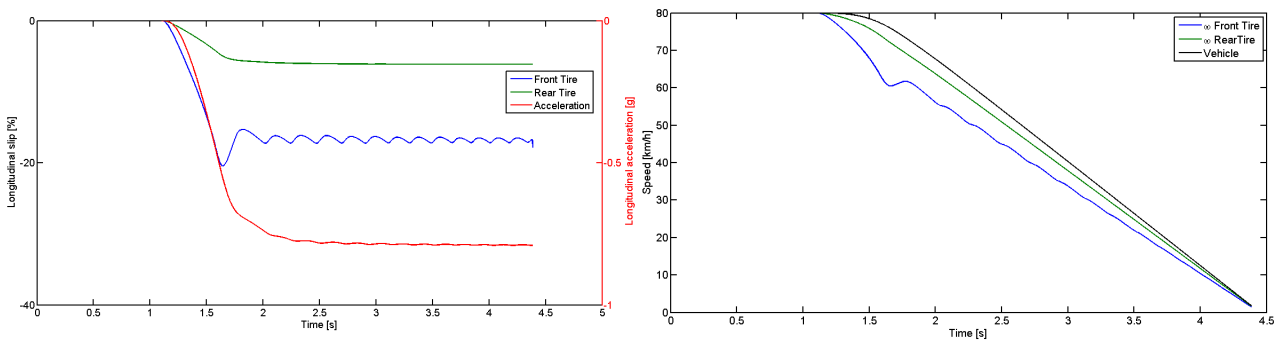


Figure 3.10: Tyre forces vs longitudinal slip

Figure 3.10 illustrates the same phenomena but with the longitudinal slip  $\kappa$  on the x-axis. This graph has also been produced with static vertical load and for five different lateral slip angles  $\alpha$ :  $0^\circ$  (green),  $2^\circ$  (blue),  $5^\circ$  (pink),  $10^\circ$  (cyan) and  $15^\circ$  (red). The graph is plotted from  $\kappa = 0$  (free rolling) to  $\kappa = -1$  (wheel lock-up). As stated in Section 3.1, a negative  $\kappa$  will generate a negative force, hence the negative forces in the graph represent longitudinal tyre forces, whereas the positive are lateral tyre forces. The behaviour as in Figure 3.9 can be observed here, i.e. that an increase in longitudinal slip  $\kappa$  lowers the lateral force available and an increase in lateral slip  $\alpha$  lowers the available longitudinal force.

The functionality of the modelled Anti-lock Braking System is shown in Figure 3.11. The executed manoeuvre is straight line braking on dry asphalt with a standard passenger vehicle. The maximum allowed slip is here set to  $\kappa$  set at 17%. The realistic behaviour of the system is due to the limited rate of change, earlier named hydraulic lag and the limited measuring frequency of the wheel speed sensor, which calculates the longitudinal slip of the respective wheel. The reason the front tyres have higher slip than the rear tyres is that brake bias of the vehicle is set so that the rear tyres do not lock up before the front tyres due to safety reasons.



(a) Longitudinal tyre slip and braking acceleration

(b) Wheel speeds

Figure 3.11: Anti-lock Braking System

The trajectory- and yaw rate plots for two different vehicles, and their corresponding reference vehicles, are shown during a cornering manoeuvre in Figures 3.12 and 3.13. The manoeuvre is performed by initially travelling in a straight line at 60km/h and after 1 second, ramping up the steering wheel from  $0^\circ$  to  $50^\circ$  during 0.5 seconds. The manoeuvre ends after 20 seconds of simulation. Neither the brake- or throttle pedal are actuated during the manoeuvre. The test is performed with two similar standard passenger vehicles, and for the sake of this demonstration they have equal cornering stiffnesses front and rear.

The difference between the two vehicles is that the first one, shown in Figure 3.12 has a weight distribution of 53% front and 47% rear. This results in an understeer gradient of  $K_u \approx 0.00162$ , according to Equation 3.40. The vehicle displayed in Figure 3.13 has the opposite, a weight distribution of 47% front and 53% rear, resulting in an understeer gradient of  $K_u \approx -0.00162$ , meaning that it is oversteering.

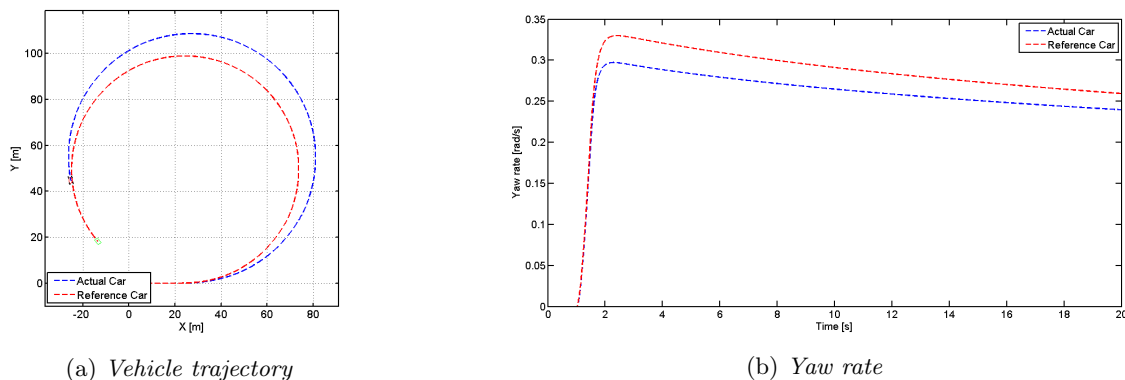


Figure 3.12: *Understeering vehicle*

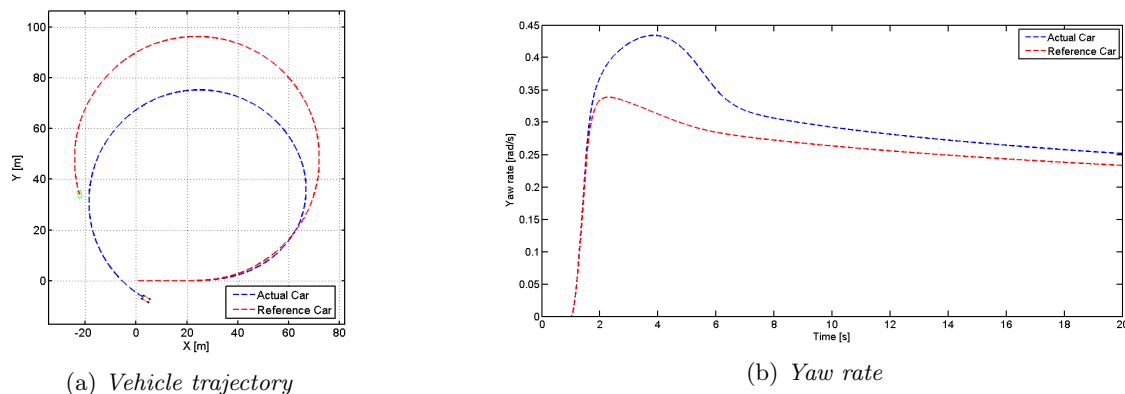


Figure 3.13: *Oversteering vehicle*

It is clear that the reference yaw rate is useful for capturing under- and oversteering behaviour as the figures above show. The vehicle with positive  $K_u$  is not cornering as much as the reference vehicle and the vehicle with negative  $K_u$  generates too much yaw rate, almost becoming unstable at the beginning of the manoeuvre. Should a control function significantly affect the cornering capability of a vehicle, the reference yaw rate is an effective way of capturing it. Criteria could be set on the RMS-value of the yaw rate error, the maximum yaw rate error or even the maximum or minimum displacement in X or Y compared to a reference vehicle.

The reason for the yaw rates decreasing over time in the plots is that the longitudinal speed is decreasing. Even though there is no rolling resistance modelled, the longitudinal friction (in the vehicle coordinate system) of the lateral forces slow the vehicle down, according to Equation 3.1. There is also a longitudinal slip created while cornering, producing longitudinal tyre forces but of very little significance in this case.

## 4 Design of Experiments

When simulating vehicles with variable parameters, the parameter limits define a space. With three variables this space becomes three-dimensional, i.e. a cuboid. The volume of this cube can be thought of as an infinite amount of unique points, containing every possible combination of parameters, which form the population. As it would be impossible to simulate each individual in the population some sort of selection of sample points has to be made. This selection should also be statistically motivated.

The approach for this thesis is to generate a population that covers the space as good as possible while keeping the sample points to a minimum. This is done to try to make sure that there is no subspace of the population where there are parameter combinations that create dangerous or unpredictable vehicle behaviour together with the control function. Also, the sampling method should be independent of the results from the simulations so that it is generic and can be used to verify any control function. Hence, all of the sample points are generated before the simulations are initialised. Another way to do it might be to treat it as an optimization problem and create an adaptive sampling method that depending on the results from the last simulation chooses a new sampling point that moves towards a defined optimum. In this thesis however no such optimum is sought after and it is also thought that this sampling method would become too dependent on which control function is currently being verified. This approach would also be much more time consuming.

### 4.1 Statistical Sampling

The statistical sampling here strives to select a subset of individuals whose characteristics represent that of the population. This includes both how to select individual sample points and to determine the amount of points needed. As stated previously the aim is to cover as much of the space as possible while maintaining a small enough sample that it is still time efficient to simulate. The three most widely used ways of doing this are random sampling, full factorial sampling and Latin hypercube sampling.

Random sampling relies on a random number generator which means that every point in a space is equally likely to be selected each time, without taking the previously generated sample points into account. Nine points sampled in a two dimensional plane might be spaced as in Figure 4.1.

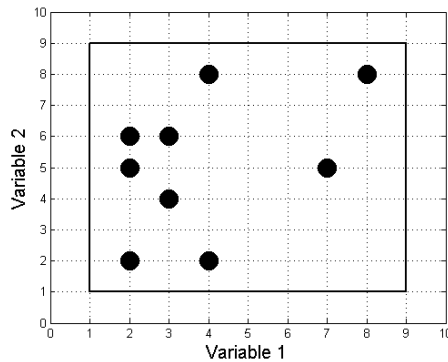


Figure 4.1: *Randomly generated samples*

As can be seen in Figure 4.1 the sample points can become concentrated in a small area, meaning that a lot of information is lost in the empty space where there are no samples.

Full factorial sampling creates  $n^D$  sample points with all possible combinations of  $n$  discrete steps in  $D$  dimensions. Three steps on two dimensions would create nine sample points placed as shown in Figure 4.2.

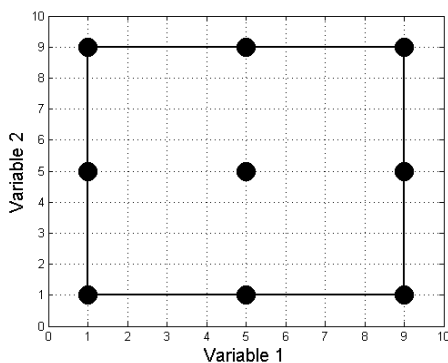


Figure 4.2: *Full factorial sample*

Full factorial always catches the boundary values of the variables as well as their combinations which can be good since the extremes are most likely to cause issues. However it leaves large gaps between its sample points and therefore might miss sensitive portions of the population.

Latin hypercube sampling (LHS) however distributes the sample points in such a way that each point has a different value of each variable. The theory is based on the Latin square which is an  $n \times n$  array filled with  $n$  different symbols, each occurring exactly once in each row and column. For the Latin hypercube it is reduced so that there is only one sample point in each row and one in each column, as shown in Figure 4.3.

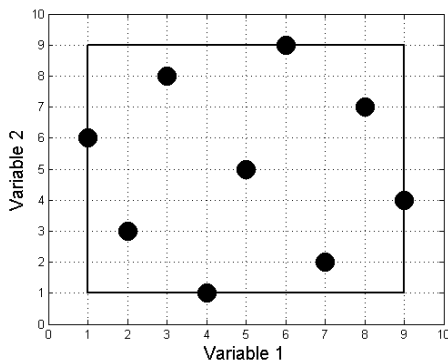


Figure 4.3: *Latin hypercube sample*

There is still some randomness with LHS as to where the sample points are placed. That means that two samples will not be identical even if LHS is given the same input twice and not always be as symmetrical as in Figure 4.3. Therefore it is also preferable to introduce a condition that seeks to maximize the minimum distance between two points, thereby increasing how much space is covered. While LHS has this randomness and is worse at finding boundary values it has much smaller steps between variable values in each dimension. This step size does not change when adding variables, which it does when using full factorial, meaning that LHS is more likely to find sensitive portions of the population, especially as the number of dimensions increases.

### 4.1.1 Evaluation of Sampling Methods

To evaluate and compare the three sampling methods they were used to generate one sample each with 64 sample points on two variables with values between 0 and 1 (this was done using Matlab). Specifics on how the samples were generated in Matlab can be found in Appendix B.

A comparison was made as to how well the different sampling methods cover the sampling interval for each variable. To visualise this, histograms were made with 64 bins for each variable meaning that for a perfectly distributed sample there should be one sample point in each bin. The results are shown in Figure 4.4. Note that there are different scales for the different methods with full factorial having eight sample points in each bin and Latin hypercube at most two (an ideal Latin hypercube only has one sample point in each bin).

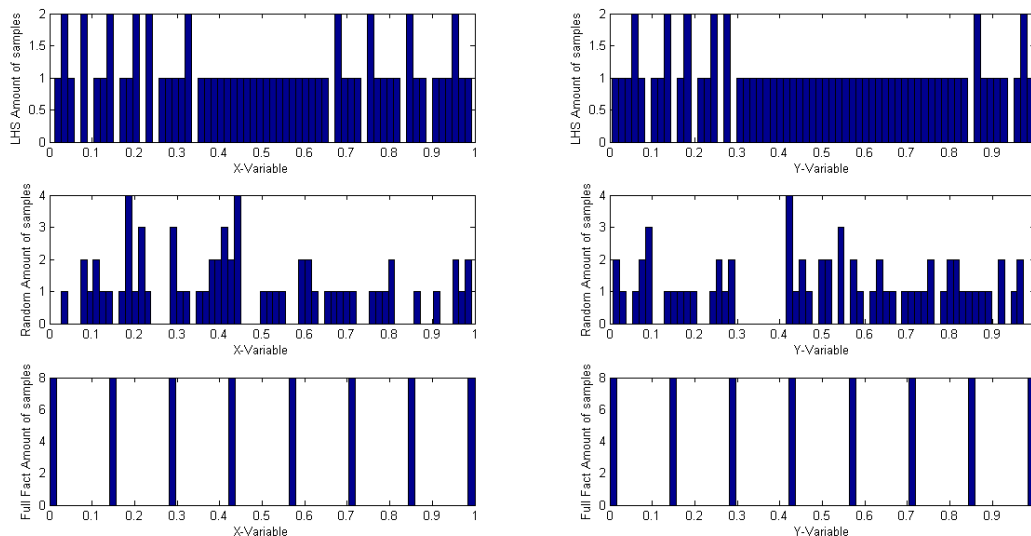


Figure 4.4: Histograms that show sampling distribution for *lhsdesign*, *rand* and *fullfact*

It quickly becomes evident that *lhsdesign* has the most well distributed sampling points and *fullfact* by far the worst. *rand* is more unpredictable and can create a good sample but also a terrible one. It has no real advantages compared to *fullfact* and *lhsdesign* and will therefore not be evaluated further.

## 4.2 Sample Size

The idea with using design of experiments is to reduce the sample size and to be able to run as few simulations as possible and still be able to rely on the results, meaning that an increase in the number of simulations would not change the results. The needed sample size, i.e. the number of simulations needed, depends highly on the number of parameters that are varied. Adding variables will add dimensions to the space that the sampling should cover. The effect of adding dimensions can be demonstrated quite well by taking full factorial as an example. If a population size of 1000 samples is considered in one dimension there will be one sample every 0.1%. If the population size is kept constant but a dimension is added there will only be about 32 different values for each variable which means that there is more than 3% between each sample point. Taking it one step even further and adding a third dimension there will only be 10 values for each parameter, meaning 10% in between. As stated before LHS is not affected in this way by adding dimensions, however there is still a risk of leaving portions of the space unsampled and as such the number of samples needed increases with increase in dimensions. The conclusion being that the only drawback with using LHS would be the ability to find extremes, however the advantages of its superior coverage and lesser dependence on number of dimensions were considered to outweigh the disadvantage and it was chosen as sampling method.

### 4.2.1 Convergence of Results

In order to analyse the number of simulations needed using LHS an empirical statistical analysis was devised. The basic principle behind this analysis was to find at what number of simulations the results converged toward a "correct" value. The simulations were run with one, two and three varying parameters. The parameters were selected as mass, weight distribution and centre of gravity height. Vehicle combinations were then selected using *lhsdesign* and they were then simulated using the vehicle model described in Chapter 2. The results from the simulations were then evaluated using criteria with specified limits for what is a passed run. What was then compared between the different runs were the percentage of vehicles that failed these criteria. Convergence was defined as the point where the variation of the percentage of failures becomes less than (and stays less than) 1%.

The results from this analysis is presented in the below figures, starting with only varying mass in Figure 4.5.

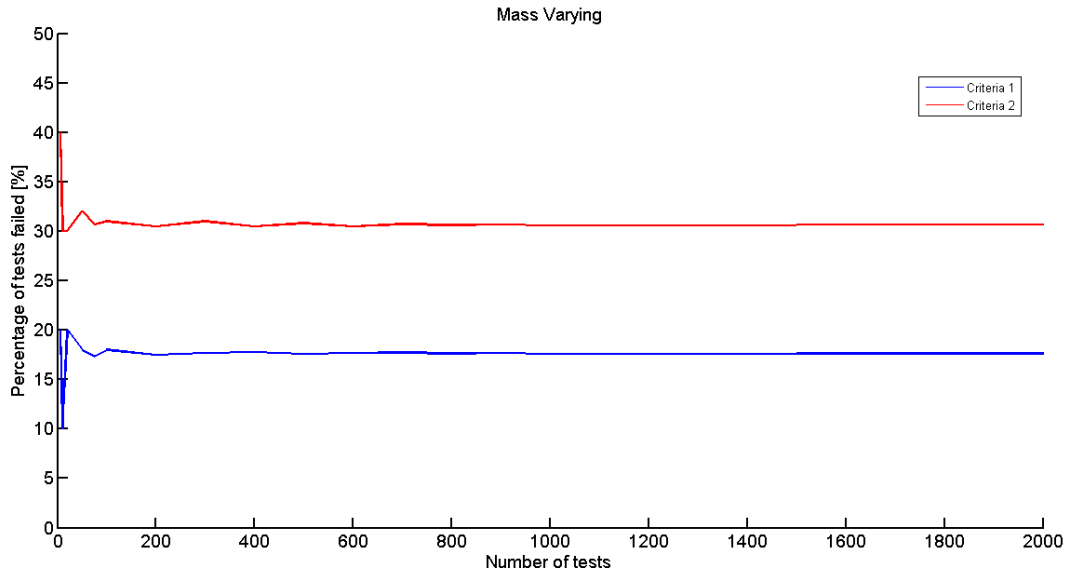


Figure 4.5: *Convergence of results with only varying mass*

The figure shows that the results converged towards a value as early as around 200 simulations. This is confirmed by the table presented in Appendix D where it can be seen that the same analysis was also done but with varying center of gravity height instead, yielding the same result (convergence at 200 simulations). Adding a dimension and varying both mass and weight distribution resulted in a graph that was a bit more unstable in the beginning as shown in Figure 4.6. In the two dimensional case the results converge at around 900 simulations. Again, the complete results are presented in Appendix D and the analysis was also done with varying mass and centre of gravity height which resulted in the same number of simulations for convergence.

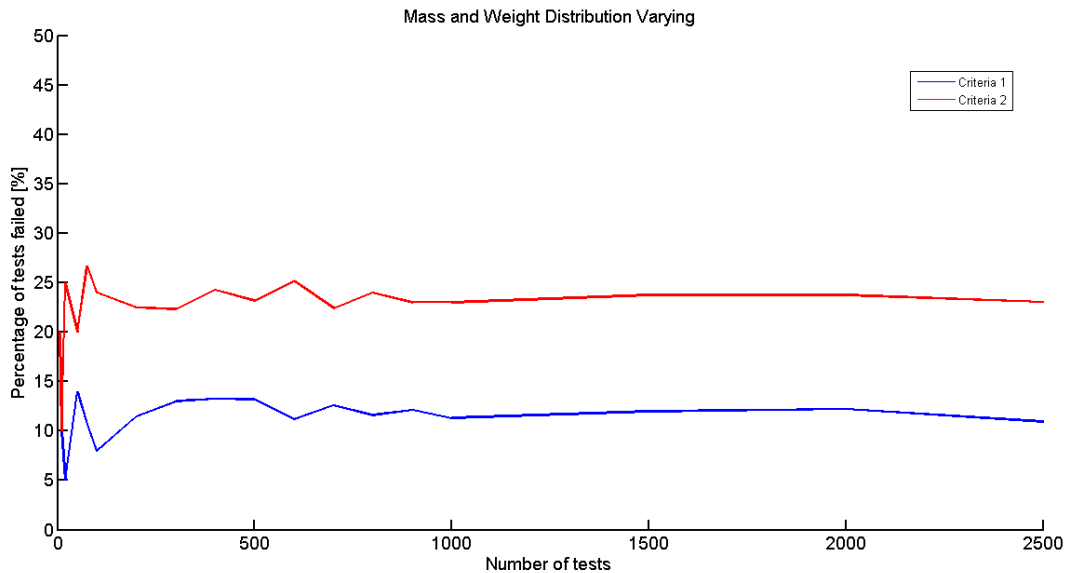


Figure 4.6: *Convergence of results with varying mass and weight distribution*

Figure 4.7 shows how adding a third dimension made the graph quite a bit more unstable and convergence did not occur until at 2500 simulations, a big increase from the 900 that two variables required. The resulting number of simulations required were compiled in a graph that describes how many simulations are needed

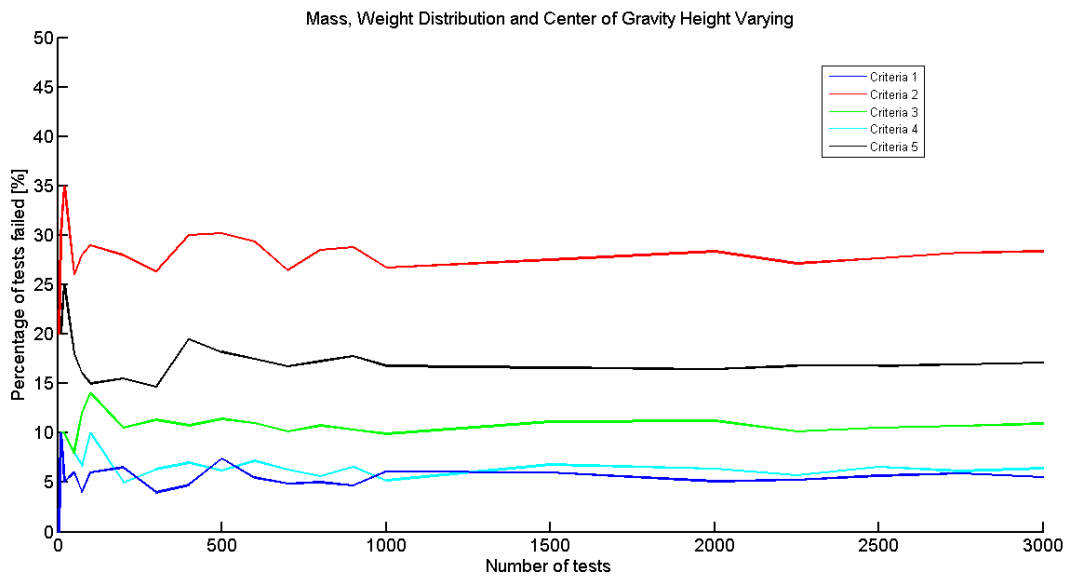


Figure 4.7: *Convergence of results with varying mass, weight distribution and center of gravity height*

depending on how many parameters that are to be varied. Figure 4.8 gives values for one, two and three parameters but might also give an indication as to how many would be needed if more parameters were to be varied.

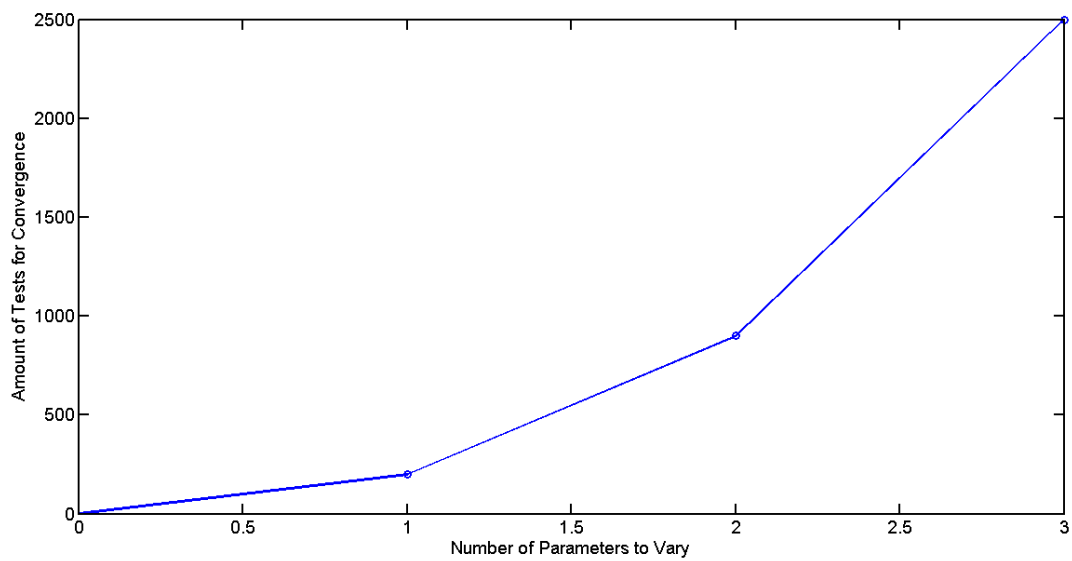


Figure 4.8: *Compiled results from convergence analysis*

## 5 Use Case: Regenerative Braking

To investigate the effectiveness and the utility of the model-in-the-loop test bench, in vehicle simulations, a use case was devised. The idea was to simulate a development process using MIL, with LHS taking a big part. What was to be developed was a regenerative braking control function, the functionality of which is described in Section 5.1. The control function was to be evaluated for a specific vehicle, a SAAB 9-3, but that did not mean that parameters such as mass and weight distribution could not vary. Since the vehicle could still be loaded in an infinite number of ways these parameters could also change accordingly. The starting point for the development was three strategy concepts called Rudimentary-, Steering Dependent- and Brake Slip Dependent regenerative braking respectively. The performance of these concepts were to be evaluated in manoeuvres judged to be critical to a control function that alters the brake moments of a vehicle; braking in a turn and straight-ahead braking on split coefficient of friction surfaces, which will be referred to as braking on split- $\mu$ .

### Model-In-the-Loop Test Bench

The MIL test bench is a software that, with some modifications, could be used to evaluate the performance of just about any control function that affects the dynamic behaviour of a vehicle. The following chapter will be a simultaneous description of the development process of the use case and how the test bench works, how it was used and how it contributed to the process. A graphical user interface was developed in order to simplify pre- and post processing; choosing parameters to vary, what manoeuvres to run and which results to look closer at etc., this will also be described more in detail as the use case unfolds.

### 5.1 Regenerative Braking

As stated before, a regenerative braking control function was to be developed. A regenerative brake is a mechanism that slows a vehicle down by converting kinetic energy into electrical and stores it in a battery, that way the energy is not dissipated as heat as with conventional friction brakes. This makes it desirable in hybrid and electrical cars as it can increase their range. It is also easily applicable in such vehicles since the required components are already there; the electrical motor is used "backwards" as a generator and the energy is stored in the same battery used normally.

Regenerative braking can be implemented in several different ways but it is very dependent on the drive train configuration used. Here a front wheel driven car with one electrical motor acting on both front wheels through a differential is considered. That means that the added brake force from the regenerative braking only applies to the front wheels, which effectively changes the brake bias of the vehicle. Also, since a differential is used the same brake moment will be applied to both wheels (select low).

#### 5.1.1 Three Strategy Concepts

The concept for control of the regenerative braking function called Rudimentary is described as a "stupid" strategy as it does not consider the behaviour of the vehicle but only its own actuation, controlled by the brake- and accelerator pedals. It has two parts, one that is called brake regen which activates when the brake pedal is pressed down and is ramped up to a certain value where it is kept constant. The other is called coast regen and is activated when the accelerator pedal is released above a threshold and ramped up to a magnitude where it is also kept constant. The actuation of the two other strategies is controlled in the same manner but they are limited by other factors as well. The Steering Dependent strategy limits the maximum brake retardation by using a feed forward from the steering angle described by Equation 5.1, an example of a limiting curve is presented in Figure 5.1

$$T = \left( 1 - \frac{\delta_f^2}{\delta_{lim}^2} \right) \cdot T_{desired} \quad (5.1)$$

The third and final strategy, Brake Slip Dependent, utilizes a feed back trigger from the ABS system which acts as an on and off switch. Essentially it turns of the regeneration when the ABS is activated. It also has a rate limiter to avoid too quick fluctuations.

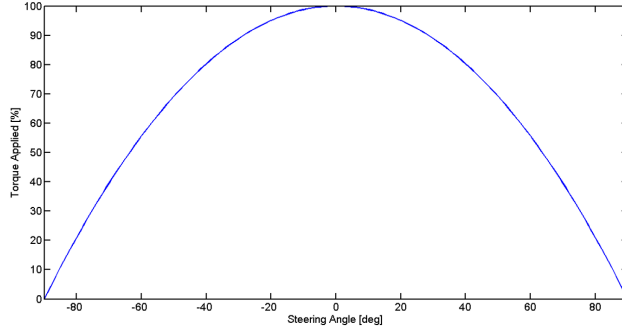


Figure 5.1: *Percentage of applied torque vs. steering wheel angle*

## 5.2 Test Matrix

As concluded in the analysis of the sampling methods Latin hypercube sampling was to be used in order to reduce the infinite test matrix created by varying vehicle parameters, environments and manoeuvres. However, for this use case the manoeuvres were limited to two and the environment was made part of those manoeuvres which meant that all vehicle combinations could be run in each manoeuvre. Therefore LHS was only used to generate the vehicle combinations. The parameters that were to change for the different vehicle combinations were limited to mass, weight distribution and center of gravity height. These are parameters that are highly affected by the loading of the vehicle and as such are subjected to frequent and diverse change.

### 5.2.1 Specification of Parameters

The basic vehicle parameters for the SAAB 9-3 were taken from the same model as was described in section 3.2 and they are listed in Appendix A. However, the limits for the varying parameters were still needed to be found/calculated. The limits for mass, weight distribution and the lower one for center of gravity height were taken from a document describing a testing procedure with a SAAB 9-3 [1]. The maximum center of gravity height however had to be calculated using the information provided in this document together with approximations of how much is loaded where etc. A combined center of gravity height is calculated as shown in Equation 5.2.

$$h_{tot} = \frac{1}{m_{tot}} \sum_{i=1}^n m_i h_i \quad (5.2)$$

For the calculation a vehicle at curb weight was loaded with a driver, a full roof box and the rest of the allowed load in the trunk, resulting in a center of gravity height of 0.73 m. The complete set of vehicle parameter limits are presented in Table 5.1.

Table 5.1: Vehicle parameter limits

	Min	Max
Mass	1510 [kg]	2155 [kg]
Weight Distribution	40.2 [% rear]	47.6 [% rear]
CoG Height	0.5 [m]	0.73 [m]

These parameter limits were then input in the graphical user interface previously mentioned, as shown in Figure 5.2.

### 5.2.2 Creation of Test Matrix

The Matlab command `lhsdesign` was used to generate a normalized test matrix with as many columns as there were parameters to be varied and as many rows as there were tests to be run. This then had to be translated

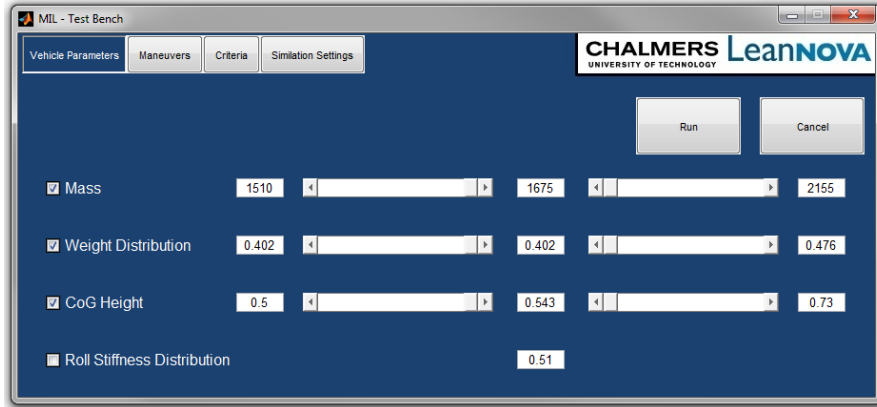


Figure 5.2: *Specification of vehicle parameter limits*

into a test matrix with a column of values for each parameter. How that was done is described in Equation 5.3 where  $\mathbf{k}$  is a column vector from the normalized test matrix (with values ranging from 0 to 1),  $\mathbf{x}$  a column vector with values for a parameter and  $x_{min}$  and  $x_{max}$  are lower and upper limits for that parameter.

$$\mathbf{x} = x_{min} + (x_{max} - x_{min})\mathbf{k} \quad (5.3)$$

### 5.3 Manoeuvres

As mentioned before the used case is defined for two manoeuvres; braking in a turn and braking on split- $\mu$ . They are both based on Swedish Standards which were used to set the conditions for the manoeuvres. For braking in a turn the initial conditions were specified in [3] as follows.

Table 5.2: Initial conditions for braking in a turn

Condition	Radius [m]	Lateral acceleration [m/s <sup>2</sup> ]	Corresponding longitudinal velocity [km/h]
Standard	100	5	81

Steady state cornering is to be achieved with the conditions specified in Table 5.2. The deceleration should then be increased in steps, starting from 2 m/s<sup>2</sup>, up to the point where all wheels lock. The standard is designed for testing of braking systems and not stability which was the point here, also the vehicle parameters change which changes the point at which the wheels lock, therefore the target braking acceleration was set to 5 m/s<sup>2</sup> (which will mean wheel lock for some but not all vehicle combinations). For braking on split- $\mu$  the procedure is rather similar but the only initial condition is that the vehicle shall be driving straight ahead at a constant velocity of 80 km/h, as specified in [2]. After reaching the steady state conditions release of the accelerator pedal and actuation of the brakes should take place as quickly as possible and the braking procedure shall be carried out with maximum deceleration. The target braking acceleration was set to 8 m/s<sup>2</sup> for braking on split- $\mu$ .

The manoeuvre conditions were specified in a separate script where they were given names and properties. The GUI then allows for selection between specified manoeuvres during preprocessing as shown in Figure 5.3. In this tab of the GUI the choice for which regenerative braking strategies should be run was also made. Any combination can be run but running without "regen off" limits the criteria as will be made clear in Section 5.4.

### 5.4 Criteria

To be able to assess the performance and/or safety of a specific run some criteria needed to be defined to be used when evaluating. Given that the chosen manoeuvres targeted different areas of vehicle stability the criteria would also have to be different for each of them. The criteria were also divided into two categories; absolute

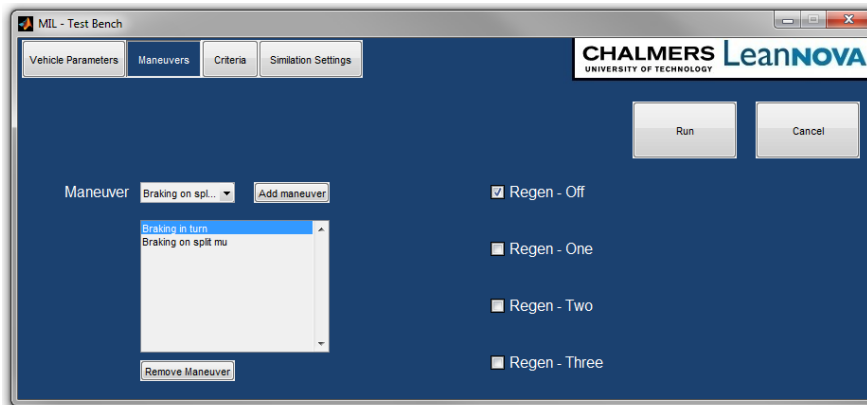


Figure 5.3: Selection of manoeuvres

criteria and relative criteria. The absolute criteria were fixed limits on vehicle behaviour while relative criteria were limits on a comparison between a specific regenerative braking strategy and the same vehicle run without regenerative braking. This means that the vehicle was not allowed to behave in certain ways but also that a regenerative braking strategy was not allowed to cause too much of a deterioration of the vehicle performance. Figure 5.4 visualizes the difference.

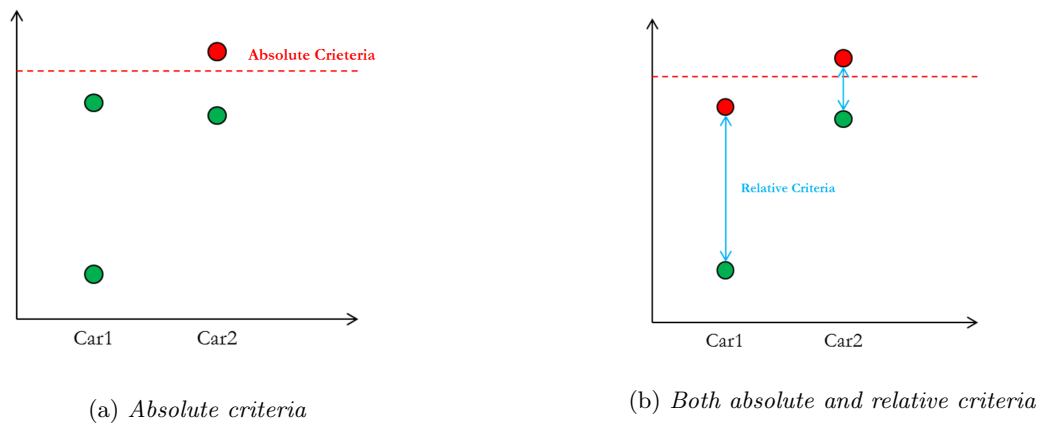


Figure 5.4: Difference between absolute and relative criteria

For braking in a turn it was considered that the absolute criteria should determine whether the car oversteers or understeers excessively, whether the braking deceleration is sufficient and there was also a criteria for wheel lift off since the vehicle model was not made to account for it. The relative criteria should determine if the regenerative braking strategies impairs the turning and braking capabilities of the vehicles. When braking on split- $\mu$  the conditions are different and therefore the criteria have to be as well, however it is still a braking manoeuvre and an absolute criteria was set for the braking acceleration. It was considered important that the yaw acceleration of the vehicle was not too high so that the driver would have time to compensate with the steering wheel. Relative criteria were also introduced for both, i.e. the regenerative strategies were not allowed to increase the yaw acceleration or decrease the braking acceleration too much. The full list of criteria for both manoeuvres are presented in Table 5.3. It should be noted that these are not in any way investigated in real life but merely example values that produced reasonable results for the given use case.

The graphical user interface gives a short description for each criteria and allows for full customization of those defined for each manoeuvre as Figure 5.5 shows (addition of criteria is handled in a separate script). For a more thorough description of the different criteria and how they are calculated see Appendix C.

Table 5.3: List of criteria

	$r/a_y$ [rad·s/m]	$RMS(r_{err})$ [rad/s]	$\bar{a}_x$ [m/s <sup>2</sup> ]	$\dot{r}_{max}$ [rad/s <sup>2</sup> ]	$\dot{r}_{max}/\dot{r}_{max_{noreg}}$ [%]	$\bar{r}/\bar{r}_{noreg}$ [%]	$\bar{a}_x/\bar{a}_{x_{noreg}}$ [%]
Braking in a turn	< 0.08	< 0.2	> 4.1			> 85	> 100
Braking on split- $\mu$			> 0.24	< 0.59	< 110		> 100

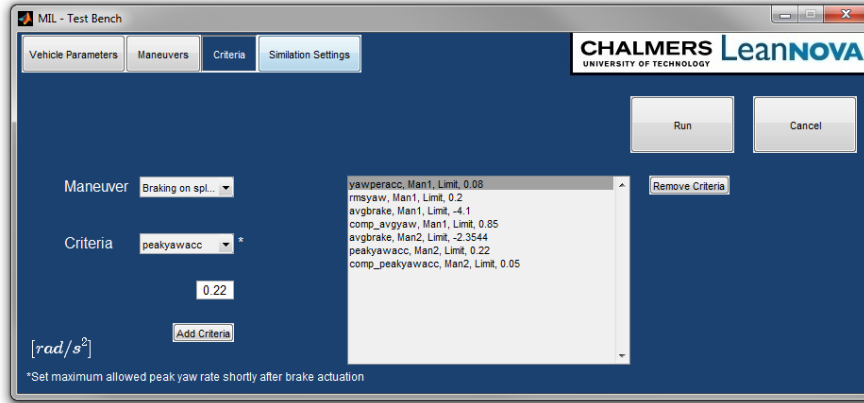


Figure 5.5: Selection of criteria

## 5.5 Initialization of Simulation

With parameters to vary, manoeuvres, and criteria chosen and specified the test bench was ready to perform the vehicle dynamics simulations with just a few more inputs. These are defined in the Simulation Settings tab as shown in Figure 5.6. The parameters the user is able to define are:

### Max simulation time [s]

The time at which each simulation is aborted regardless of what happens in the model

### Sample time [s]

The step size used in the simulations

### Vehicle combinations

The number of vehicle combinations that are to be generated in the test matrix

The max simulation time is often not used since the vehicle model interrupts when the velocity goes towards zero, however it is set to 20 s so that the simulation aborts even when there is an error. The sample time is set to 0.001 s because of reasons described in Section 3.3. The first run of the use case was done to get an idea of how the regenerative braking strategies affected the vehicle behaviour in the two manoeuvres. This relative comparison with the same vehicles did not demand the high number of vehicle combinations proposed in Section 4.2 even though three vehicle parameters were varied. Vehicle combinations was therefore set to just 100.

## 5.6 Evaluation

The high amount of results that are calculated in the vehicle model together with the fact that several thousand vehicles can be simulated at once makes the evaluation process rather difficult. For this reason a script was written that would compare results from the simulations with specified criteria and generate a data structure in Matlab as well as a results report in excel. An additional post-process GUI was also developed that would

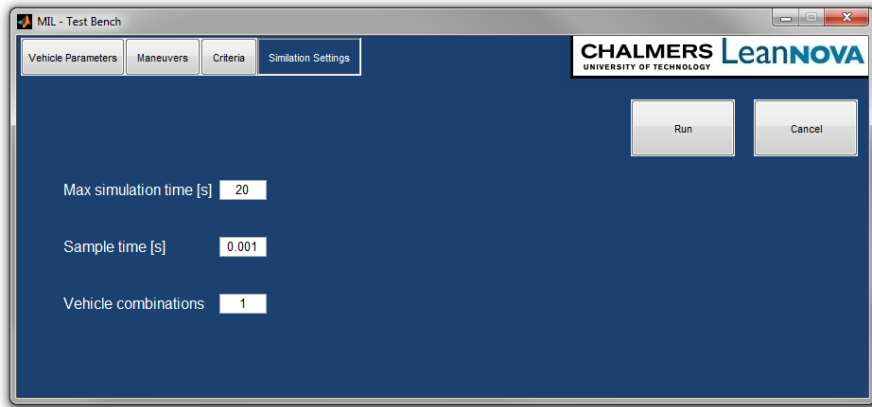


Figure 5.6: *Specification of simulation parameters*

let the user access basically all the data from the simulations easily and with a good overview, without having to dig through the data structure manually. All of the data from every simulation is not saved but merely the results related to the criteria and some vehicle parameters. When the user wants to access more in depth data from a certain simulation it is run individually and the results are added to the data structure (one simulation taking approximately one second).

## 5.7 Results Generation

When the whole test matrix is simulated the test bench makes the results available in a number of different ways. As mentioned above it generates a results report and a GUI that helps the user sort through the data structure. The first thing that pops up however is a general overview of passed and failed tests as shown in Figure 5.7. One histogram is made for each manoeuvre, displaying the percentage of vehicles that failed any criteria for each regenerative braking strategy, numbered from one to three as in Subsection 5.1.1. The vehicles assessed in these plots are only those which passed all criteria with regenerative braking turned off. The reason for this is that when generating the test matrix as described in Subsection 5.2.2 some unrealistic vehicle combinations can be created, e.g. the program does not prohibit that a vehicle has minimum mass in combination with the highest center of gravity height. This would be impossible in reality since it is an addition of mass that causes the increase in center of gravity height. Thus, vehicles that fail any criteria without a regenerative braking strategy active was considered to be unrealistic and removed.

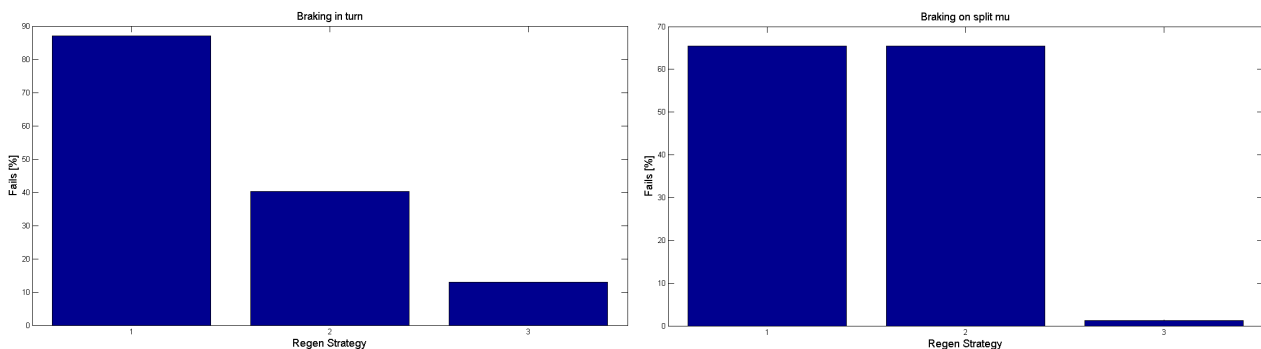


Figure 5.7: *Overview of percentage of vehicles that failed*

Figure 5.7 shows the actual results from the first run in the use case. It can quickly be seen that the Rudimentary strategy has very high fail percentages in both manoeuvres. The second strategy, Steering dependent, however behaved reasonably well in braking in a turn but just as poorly as Rudimentary when braking on split- $\mu$ , since the steering wheel angle is zero. The Brake slip dependent strategy had the lowest amount of fails for both manoeuvres, this might lead to the conclusion that it is always better. However, further analysis of the results were needed before drawing such conclusions, starting with the results report.

## Results Report

The results report is presented in excel as shown in Figure 5.8 and provides a bit more in depth information, however it is not opened automatically. The report is divided into sheets where there is one for each combination of regenerative braking strategies and manoeuvres. This means that with four strategies (including no regenerative braking) and two manoeuvres, eight sheets are created. It then presents the vehicle combinations, one on each row, and how they performed when evaluated towards each criteria, as well as the total percentage that failed. It also provides a list of which vehicle combinations failed when the one without regenerative braking passed. When analysing this list for the use case it was found that a few vehicles that failed with the Braking dependent strategy actually passed with the Steering dependent, suggesting that the Brake slip dependent is not always superior.

	A	B	C	D	E	F	G	H	I	J	K
1		Rudimentar	rmsyaw	yawperacc	avgbrake	rmax	WLOF	peakyawacc	comp_peakyawacc	comp_avgyaw	comp_avgbrake
2	Percentage failed	90%	0%	19%	0%	0%	0%	0%	0%	90%	0%
14	Car12	X	✓	✓	✓		✓			X	✓
15	Car13	X	✓	✓	✓		✓			X	✓
16	Car14	X	✓	✓	✓		✓			X	✓
17	Car15	X	✓	✓	✓		✓			X	✓
18	Car16	X	✓	✓	✓		✓			X	✓
19	Car17	X	✓	✓	✓		✓			X	✓
20	Car18	X	✓	X	✓		✓			X	✓
21	Car19	X	✓	✓	✓		✓			X	✓
22	Car20	X	✓	✓	✓		✓			X	✓
23	Car21	X	✓	✓	✓		✓			X	✓
24	Car22	✓	✓	✓	✓		✓			X	✓
25	Car23	X	✓	✓	✓		✓			X	✓
26	Car24	X	✓	✓	✓		✓			X	✓
27	Car25	X	✓	X	✓		✓			X	✓
28	Car26	✓	✓	✓	✓		✓			X	✓
29	Car27	X	✓	✓	✓		✓			X	✓
30	Car28	X	✓	✓	✓		✓			X	✓
31	Car29	X	✓	X	✓		✓			X	✓
32	Car30	X	✓	✓	✓		✓			X	✓
33	Car31	X	✓	X	✓		✓			X	✓
34	Car32	X	✓	✓	✓		✓			X	✓

Figure 5.8: Results report in Excel

## Post-processing Graphical User Interface

Apart from the histograms described in Subsection 5.7 the graphical user interface developed for post-processing also opens automatically when all of the the simulations are finished. This user interface has three tabs with different plotting tools, the first of which is shown in Figure 5.9. The others are used for single vehicle plots and single vehicle trajectory. It also has a fourth tab called Re-evaluation, which allows for redefinition of criteria. This was introduced in order to avoid having to re-run all of the simulations if it is found that a criteria was defined incorrectly.

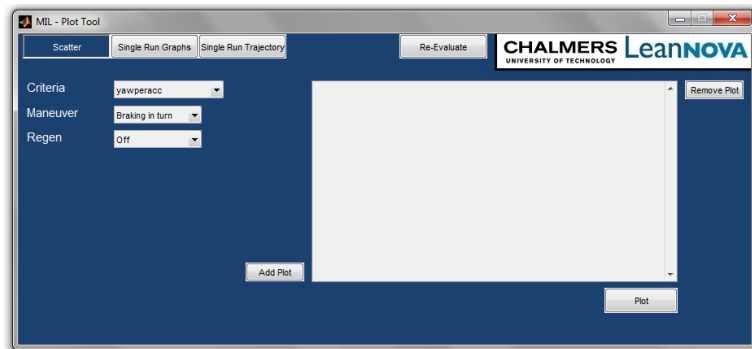


Figure 5.9: Post-process graphical user interface - Scatter

## Multi-vehicle Scatter plots

This tab is used for creating scatter plots for a certain criteria, manoeuvre and regenerative strategy selected by the user, each vehicle combination is represented by a number which is printed in green if that vehicle passed the specific criteria and red if not. The criteria limit is also shown as a dashed red line. An example of a scatter plot from the use case is shown in Figure 5.10 which is specifically for the Rudimentary regenerative braking strategy in the first manoeuvre, braking in a turn. The criteria is the relative criteria for average yaw rate, which was, as Figure 5.10 visualises, the criteria where most of them failed. As can be seen in Appendix C this criteria is defined as the percentage of yaw rate that is maintained after the brakes are applied.

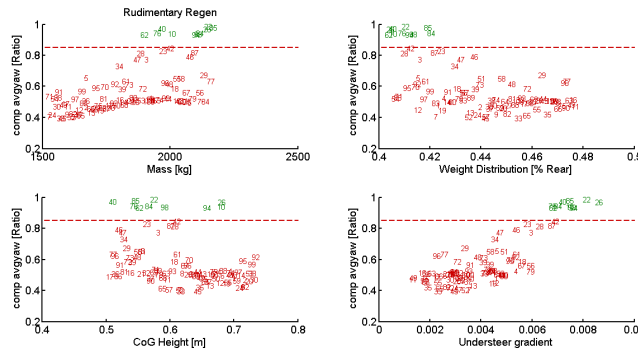


Figure 5.10: Scatter plot, example from use case

## Single Vehicle Plots

To investigate why it is that so many of the vehicles with the Rudimentary strategy failed on that specific criteria it is possible to use single vehicle plots, displayed in Figure 5.11.

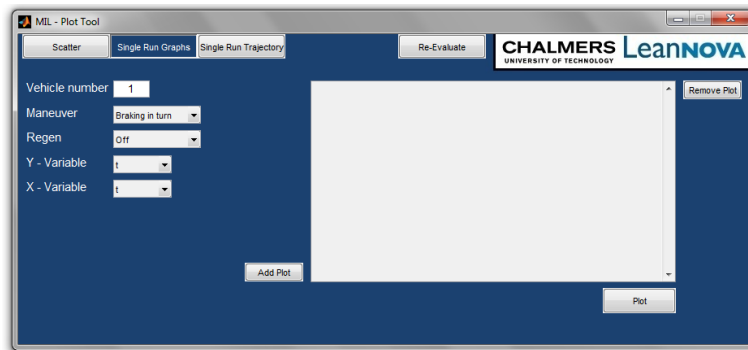


Figure 5.11: Graphical user interface - Single run graphs

Here the user selects a vehicle number, manoeuvre, regenerative braking strategy and what to plot. It is possible to plot several graphs in the same figure by adding them to the list. For the use case, it was desired to further visualise how the yaw rate varied over time for the different strategies to see what made the Rudimentary regenerative braking fail the relative criteria for average yaw rate.

Figure 5.12 shows that the car with the Rudimentary regenerative braking has a big dip in yaw rate right after the brakes were applied (6.5 s) which caused it to fail the criteria. The same tab in the user interface was then used to investigate the wheel slip of the vehicle in question and it was realised that the wheels lock up almost immediately after brake actuation which reduces the lateral grip causing the vehicle to lose yaw rate.

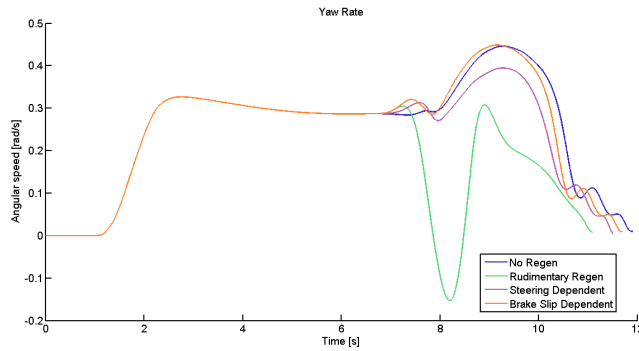


Figure 5.12: *Yaw rate comparison between regenerative braking strategies*

### Single Vehicle Trajectory

In the single vehicle trajectory tab the user again selects a vehicle number, manoeuvre and regenerative braking strategy. An animation of the vehicle trajectory is then displayed which can be useful to get a first understanding of how the vehicle behaves. It simultaneously animates a reference trajectory using the reference yaw rate described in Section 3.2.1 which helps to show whether the vehicle is over- or understeering.

## 5.8 Improvement and Iteration

The conclusions drawn from the work described in the previous sections were that the Rudimentary strategy was much worse than the other two and would therefore not be considered for further development. The Brake slip dependent strategy was the one that performed best by far but it was also seen that it failed on some vehicles where the Steering dependent did not. Because of this it was decided to create a combination of the two; a strategy that was both steering and brake slip dependent. This was then implemented as the new first regenerative braking strategy, replacing Rudimentary. A new batch of simulations was initiated with the same parameters to vary, the same manoeuvres, the same criteria and again with only 100 vehicle combinations just to be able to compare. The first overview of the results are presented in Figure 5.13. The percentages of vehicles that failed with the combined strategy were very low, about 4 and 2 percent.

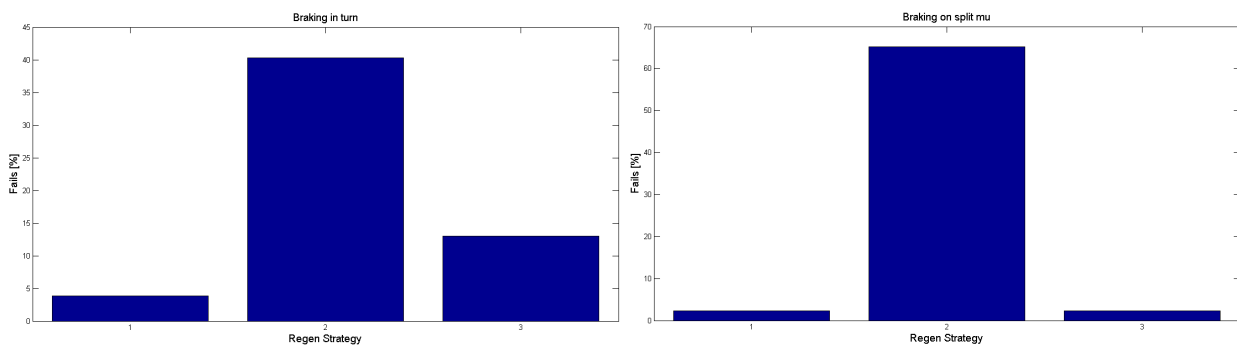


Figure 5.13: *Overview of percentage of vehicles that failed*

## 5.9 Final Strategy

The results in Figure 5.13 were good enough that it was deemed justified to run a new batch with only the combined strategy together with no regenerative braking, using the recommended amount of vehicle combinations (2500 with three varying parameters). As can be seen in Table 5.4 the results from the bigger batch was even better than before as the percentage of fails in both manoeuvres were one or lower and the combined strategy was selected as the final one and the use case was judged a success.

Table 5.4: Combined regenerative braking strategy, 2500 vehicle combinations

	Percentage failed vehicle combinations
Braking in a turn	1
Braking on split- $\mu$	0.7

## 6 Conclusions

The presented use case is an indicator that the developed test bench could be an effective tool in the early development process to quickly be able to compare different control functions and choose which ones to scrap and which to focus on in further development. It also has potential to be useful in those later stages of development where one function is refined and tuned by providing critical situations where hazards can occur. However, to be able to trust the results in a larger extent the vehicle model has to be verified against test data from a real vehicle to judge whether it behaves properly. If it does not the interface between the test bench and vehicle model is not complex and the model could be exchanged easily. It should be considered though that it is an advantage in these circumstances to use a rather simple vehicle model that does not require too much computing power, since it is intended to run several thousands of simulations at once. The importance of the accuracy of the results should therefore be judged against the time available during development and the model should be just advanced enough that it provides reliable information for what is being studied. If the goal, for example, is to investigate only lateral dynamics it might unnecessary to introduce rolling wheels and longitudinal slip since this highly affects the sampling frequency required without contributing to the accuracy of the lateral dynamics simulations.

During the use case it also became evident that the number of vehicle combinations heavily influences the outcome regarding failed tests. When comparing the results for the combined strategy in Figure 5.13 with those presented in Table 5.4 it can be seen that increasing the number of vehicle combinations from 100 to 2500, while keeping everything else the same, reduced the percentage failed vehicle combinations from 4% and 2% to 1% and 0.7% respectively.

## References

- [1] P. W. Broertjes. *Approval No.: E4-13-HR-000038*. May 27, 2002.
- [2] S. S. Institute. *SS-ISO 14512. Passenger cars - Straight-ahead braking on split coefficient of friction surfaces - Open-loop test procedure*. 2000.
- [3] S. S. Institute. *SS-ISO 7975:2006. Passenger cars - Braking in a turn - Open loop test method*. 2006.
- [4] S. S. Institute. *SS-ISO 8855:2011. Road vehicles - Vehicle dynamics and road-holding ability - Vocabulary*. 2012.
- [5] B. Jacobson. *Vehicle Dynamics. Compendium for Course MMF062*. Chalmers University of Technology, 2012.
- [6] Mathworks. *Speed Up Simulation*. Feb. 15, 2014. URL: <http://www.mathworks.se/help/simulink/ug/speeding-up-the-simulation.html>.
- [7] H. B. Pacejka. *Tyre and Vehicle Dynamics*. Elsevier Butterworth-Heinemann, 2002.

# Appendices

## A Vehicle Initial Parameters

$b_{bias}$	= 80% front, Brake moment distribution
$c_\lambda$	= 51% front, Roll stiffness distribution
$c_\Phi$	= 70,000 $\frac{N}{rad}$ , Total roll stiffness
$h$	= 0.543 m, CoG height from ground
$h_0$	= 0.4755 m, Height of CoG above roll axis
$h_1$	= 0.045 m, Front roll center height
$h_2$	= 0.101 m, Rear roll center height
$I_{w_{yy}}$	= 1.2 $kgm^2$ , Wheel moment of inertia about y-axis
$I_{yy}$	= 800 $kgm^2$ , Vehicle moment of inertia about x-axis
$I_{zz}$	= 2617 $kgm^2$ , Vehicle moment of inertia about z-axis
$m$	= 1675 kg, Vehicle total mass
$m_s$	= 1475 kg, Vehicle sprung mass
$m_w$	= 22.5 kg, Wheel mass
$l_1$	= 1.07535 m, Distance from CoG to front axle
$l_2$	= -1.59965 m, Distance from CoG to rear axle
$L$	= 2.675 m, Wheelbase
$k_\lambda$	= 0.56% front, Roll damping distribution
$k_\Phi$	= 8000 $\frac{N}{rad/s}$ , Total roll damping
$K_u$	= 0.00529, Understeer gradient
$n_{st}$	= 15.9, Steering ratio
$R$	= 0.3 m, Wheel radius
$w$	= 1.5 m, Trackwidth
$c_1$	= 8, Magic Tire Formula stiffness parameter
$c_2$	= 1.33, Magic Tire Formula stiffness parameter
$C_x$	= 1.5, Magic Tire Formula shape factor
$C_y$	= 1.3, Magic Tire Formula shape factor
$E_x$	= -1, Magic Tire Formula curvature factor
$E_y$	= -1, Magic Tire Formula curvature factor
$\mu_1$	= $6 \cdot 10^{-5}$ , Tyre load based non-linearity parameter for friction

## B Sampling Methods

### Random sampling

To create the random sample the built in Matlab-function *rand* was used.  $r = rand(n, m)$  returns an  $n \times m$  matrix of pseudorandom uniform values between 0 and 1<sup>1</sup>. By setting both  $n$  to 64 and  $m$  to 2 the correct sample was generated directly.

### Full factorial sampling

" $dFF = fullfact(levels)$  gives factor settings  $dFF$  for a full factorial design with  $n$  factors, where the number of levels for each factor is given by the vector *levels* of length  $n$ .  $dFF$  is  $m$ -by- $n$ , where  $m$  is the number of treatments in the full-factorial design. Each row of  $dFF$  corresponds to a single treatment. Each column contains the settings for a single factor, with integer values from one to the number of levels."<sup>2</sup>

This is how Mathworks describes the *fullfact* function in Matlab. This means that  $dFF = fullfact([p\ p])$  would create a  $p^2 \times 2$  matrix with all of the number combinations from 1 to  $p$ . To create a test matrix with 64 entries for each variable that would mean setting  $p = 8$ . Also, in this instance it was desired to fill the test matrix with numbers ranging from 0 to 1 which meant that another calculation was needed:

$$dFFF = \frac{(dFF - 1)}{(p - 1)} \tag{B.1}$$

**Example**  $dFFF = fullfact([3\ 3])$ :

$$dFF = \begin{bmatrix} 1 & 1 \\ 2 & 1 \\ 3 & 1 \\ 1 & 2 \\ 2 & 2 \\ 3 & 2 \\ 1 & 3 \\ 2 & 3 \\ 3 & 3 \end{bmatrix}$$

Using Equation B.1 with  $p = 3$  then gives:

$$dFFF = \begin{bmatrix} 0 & 0 \\ 0.5 & 0 \\ 1 & 0 \\ 0 & 0.5 \\ 0.5 & 0.5 \\ 1 & 0.5 \\ 0 & 1 \\ 0.5 & 1 \\ 1 & 1 \end{bmatrix}$$

### Latin hypercube sampling

LHS was also done using a built in Matlab function, called *lhsdesign*. " $X = lhsdesign(n, p)$  returns an  $n \times p$  matrix,  $X$ , containing a latin hypercube sample of  $n$  values on each of  $p$  variables. For each column of  $X$ , the  $n$  values are randomly distributed with one from each interval  $(0, 1/n), (1/n, 2/n), \dots, (1 - 1/n, 1)$ , and they are randomly permuted".<sup>3</sup>

<sup>1</sup><http://www.mathworks.se/help/matlab/ref/rand.html>

<sup>2</sup><http://www.mathworks.se/help/stats/fullfact.html>

<sup>3</sup><http://www.mathworks.se/help/stats/lhsdesign.html>

## C Definition of Criteria

$RMS(r_{err})$ , also referred to as 'rmsyaw' in sections where mathematical symbols are incompatible, is the root-mean-square value of the yaw rate error. The error is defined as  $r_{err} = r_{ref} - r$  where  $r_{ref}$  is the reference yaw rate according to Equation 3.41. The criteria is implemented in order to capture severe under- or oversteering vehicle behaviour. The criteria is measured in  $rad/s$  and has a maximum limit.

$r/a_y$  (**yawperacc**) is the relation between yaw rate  $r$  and lateral acceleration  $a_y$ . The value is measured at the time where the yaw rate is the highest for the manoeuvre. The criteria captures test runs where the vehicle spins, in which case the yaw rate is considerably higher than the lateral acceleration. This behaviour is not always captured by the  $rms(r_{err})$  since the values for yaw rate error during spinning is peculiar. The criteria is measured in  $rad \cdot s/m$  and has a maximum limit.

$\bar{a}_x$  (**avgyaw**) is the mean value of the braking retardation during manoeuvre, measured from the start of braking. The criteria is added to ensure that the vehicle is decelerating sufficiently. The criteria is measured in  $m/s^2$  and has a maximum limit (negative acceleration while braking).

$t_{WLOF}$  (**WLOF**) measures the time where at least one wheel is not in contact with the ground (any  $F_z < 0$ ). The vehicle model does not handle wheel lift-off very well and the criteria is introduced to warn the user that the simulation results are not reliable. The criteria is measured in seconds and has a maximum limit.

$\dot{r}_{max}$  (**peakyawacc**) is the maximum yaw acceleration between start of braking and a certain time thereafter. The criteria captures yaw increasing effects when braking in a straight line, where yaw rate is undesired, e.g. on split- $\mu$  conditions. The simulation environment does not include a driver model to countersteer, which is why the criteria is measured in a small time frame. The unit is  $rad/s^2$  and the criteria has a maximum limit on the absolute value.

$\dot{r}_{max}/\dot{r}_{max_{noregen}}$  (**comp\_peakyawacc**) compares the maximum yaw acceleration between the vehicle with the specific control function activated and deactivated respectively. The criteria is implemented to capture the cases where the control function causes an unsafe increase of yaw acceleration, compared to the vehicle with the system deactivated. This criteria is measured in % and has a maximum limit.

$\bar{r}/\bar{r}_{noregen}$  (**comp\_avgyaw**) compares the average yaw rate between the vehicle with the specific control function activated and deactivated respectively. The reason for the criteria is to capture cases where the control function decreases the cornering capability of the vehicle. The criteria is measured in % and has a minimum limit.

$\bar{a}_x/\bar{a}_{x_{noregen}}$  (**comp\_avgbrake**) compares the average braking retardation between the vehicle with the specific control function activated and deactivated respectively. The criteria is implemented to make sure that the control function does not decrease the braking capability of the vehicle. The criteria has a minimum limit, i.e. at least a certain portion of braking capability should remain, and is measured in %.

## D Samples Needed for Convergence

		Only vary mass									
		yawperacc		rmsyaw		Avgbrake		WLOF		Total	
		No fails	Perc fail	No fails	Perc fail	No fails	Perc fail	No fails	Perc fail	No fails	Perc fail
Test											
5	2	40,00%	1	20,00%	0	0,00%	0	0,00%	2	40,00%	
10	3	30,00%	1	10,00%	0	0,00%	0	0,00%	3	30,00%	
20	6	30,00%	4	20,00%	0	0,00%	0	0,00%	6	30,00%	
50	16	32,00%	9	18,00%	0	0,00%	0	0,00%	16	32,00%	
75	23	30,67%	13	17,33%	0	0,00%	0	0,00%	23	30,67%	
100	31	31,00%	18	18,00%	0	0,00%	0	0,00%	31	31,00%	
200	61	30,50%	35	17,50%	0	0,00%	0	0,00%	61	30,50%	
300	93	31,00%	53	17,67%	0	0,00%	0	0,00%	93	31,00%	
400	122	30,50%	71	17,75%	0	0,00%	0	0,00%	122	30,50%	
500	154	30,80%	88	17,60%	0	0,00%	0	0,00%	154	30,80%	
600	183	30,50%	106	17,67%	0	0,00%	0	0,00%	183	30,50%	
700	215	30,71%	124	17,71%	0	0,00%	0	0,00%	215	30,71%	
800	245	30,63%	141	17,63%	0	0,00%	0	0,00%	245	30,63%	
900	276	30,67%	159	17,67%	0	0,00%	0	0,00%	276	30,67%	
1000	306	30,60%	176	17,60%	0	0,00%	0	0,00%	306	30,60%	
2000	613	30,65%	353	17,65%	0	0,00%	0	0,00%	613	30,65%	
		Vary CoG Height									
		yawperacc		rmsyaw		Avgbrake		WLOF		Total	
		No fails	Perc fail	No fails	Perc fail	No fails	Perc fail	No fails	Perc fail	No fails	Perc fail
Tests											
5	0	0,00%	0	0,00%	0	0,00%	0	0,00%	0	0,00%	
10	0	0,00%	0	0,00%	1	10,00%	0	0,00%	1	10,00%	
20	0	0,00%	0	0,00%	1	5,00%	0	0,00%	1	5,00%	
50	0	0,00%	0	0,00%	3	6,00%	0	0,00%	3	6,00%	
75	0	0,00%	0	0,00%	6	8,00%	0	0,00%	6	8,00%	
100	0	0,00%	0	0,00%	7	7,00%	0	0,00%	7	7,00%	
200	0	0,00%	0	0,00%	16	8,00%	0	0,00%	16	8,00%	
300	0	0,00%	0	0,00%	23	7,67%	0	0,00%	23	7,67%	
400	0	0,00%	0	0,00%	30	7,50%	0	0,00%	30	7,50%	
500	0	0,00%	0	0,00%	40	8,00%	0	0,00%	40	8,00%	
600	0	0,00%	0	0,00%	45	7,50%	0	0,00%	45	7,50%	
700	0	0,00%	0	0,00%	53	7,57%	0	0,00%	53	7,57%	
800	0	0,00%	0	0,00%	63	7,88%	0	0,00%	63	7,88%	
900	0	0,00%	0	0,00%	69	7,67%	0	0,00%	69	7,67%	
1000	0	0,00%	0	0,00%	80	8,00%	0	0,00%	80	8,00%	
1500	0	0,00%	0	0,00%	116	7,73%	0	0,00%	116	7,73%	
2000	0	0,00%	0	0,00%	160	8,00%	0	0,00%	160	8,00%	

Figure D.1: Samples needed for convergence, one varying parameter

<b>Vary Weight Distribution and CoG Height</b>											
		yawperacc		rmsyaw		Avgbrake		WLOF		Total	
		No fails	Perc fail	No fails	Perc fail	No fails	Perc fail	No fails	Perc fail	No fails	Perc fail
Test											
	5	0	0,00%	0	0,00%	0	0,00%	0	0,00%	0	0,00%
	10	0	0,00%	0	0,00%	1	10,00%	1	10,00%	1	10,00%
	20	0	0,00%	0	0,00%	2	10,00%	1	5,00%	2	10,00%
	50	0	0,00%	0	0,00%	3	6,00%	2	4,00%	3	6,00%
	75	2	2,67%	0	0,00%	7	9,33%	3	4,00%	7	9,33%
	100	2	2,00%	0	0,00%	10	10,00%	3	3,00%	11	11,00%
	200	3	1,50%	0	0,00%	17	8,50%	9	4,50%	19	9,50%
	300	6	2,00%	0	0,00%	24	8,00%	11	3,67%	26	8,67%
	400	6	1,50%	0	0,00%	32	8,00%	21	5,25%	33	8,25%
	500	3	0,60%	0	0,00%	42	8,40%	29	5,80%	44	8,80%
	600	3	0,50%	0	0,00%	45	7,50%	25	4,17%	48	8,00%
	700	7	1,00%	0	0,00%	65	9,29%	36	5,14%	68	9,71%
	800	9	1,13%	0	0,00%	57	7,13%	33	4,13%	63	7,88%
	900	5	0,56%	0	0,00%	90	10,00%	56	6,22%	92	10,22%
	1000	11	1,10%	0	0,00%	94	9,40%	53	5,30%	98	9,80%
	1500	9	0,60%	0	0,00%	128	8,53%	66	4,40%	129	8,60%
	2000	20	1,00%	0	0,00%	190	9,50%	101	5,05%	198	9,90%
	2500	22	0,88%	0	0,00%	233	9,32%	136	5,44%	242	9,68%
<b>Vary Mass och Weight Dist</b>											
		yawperacc		rmsyaw		Avgbrake		WLOF		Total	
		No fails	Perc fail	No fails	Perc fail	No fails	Perc fail	No fails	Perc fail	No fails	Perc fail
Test											
	5	1	20,00%	1	20,00%	0	0,00%	0	0,00%	1	20,00%
	10	1	10,00%	1	10,00%	0	0,00%	0	0,00%	1	10,00%
	20	5	25,00%	1	5,00%	0	0,00%	0	0,00%	5	25,00%
	50	10	20,00%	7	14,00%	0	0,00%	0	0,00%	10	20,00%
	75	20	26,67%	8	10,67%	0	0,00%	0	0,00%	20	26,67%
	100	24	24,00%	8	8,00%	0	0,00%	0	0,00%	24	24,00%
	200	45	22,50%	23	11,50%	0	0,00%	0	0,00%	45	22,50%
	300	67	22,33%	39	13,00%	0	0,00%	0	0,00%	67	22,33%
	400	97	24,25%	53	13,25%	0	0,00%	0	0,00%	97	24,25%
	500	116	23,20%	66	13,20%	0	0,00%	0	0,00%	116	23,20%
	600	151	25,17%	67	11,17%	0	0,00%	0	0,00%	151	25,17%
	700	157	22,43%	88	12,57%	0	0,00%	0	0,00%	157	22,43%
	800	192	24,00%	93	11,63%	0	0,00%	0	0,00%	192	24,00%
	900	207	23,00%	109	12,11%	0	0,00%	0	0,00%	207	23,00%
	1000	230	23,00%	113	11,30%	0	0,00%	0	0,00%	230	23,00%
	1500	356	23,73%	180	12,00%	0	0,00%	0	0,00%	356	23,73%
	2000	475	23,75%	244	12,20%	0	0,00%	0	0,00%	475	23,75%
	2500	576	23,04%	274	10,96%	0	0,00%	0	0,00%	576	23,04%

Figure D.2: Samples needed for convergence, two varying parameters

Vary Mass, weight dist and CoG height												
Tests	yawperacc			rmsyaw		Avgbrake		WLOF		Total		
	No fails	Perc fail		No fails	Perc fail							
5	1	20,00%		0	0,00%	0	0,00%	0	0,00%	1	20,00%	
10	2	20,00%		1	10,00%	1	10,00%	1	10,00%	3	30,00%	
20	5	25,00%		2	10,00%	2	10,00%	1	5,00%	7	35,00%	
50	9	18,00%		4	8,00%	4	8,00%	3	6,00%	13	26,00%	
75	12	16,00%		5	6,67%	9	12,00%	3	4,00%	21	28,00%	
100	15	15,00%		10	10,00%	14	14,00%	6	6,00%	29	29,00%	
200	31	15,50%		10	5,00%	21	10,50%	13	6,50%	56	28,00%	
300	44	14,67%		19	6,33%	34	11,33%	12	4,00%	79	26,33%	
400	78	19,50%		28	7,00%	43	10,75%	19	4,75%	120	30,00%	
500	91	18,20%		31	6,20%	57	11,40%	37	7,40%	151	30,20%	
600	105	17,50%		43	7,17%	66	11,00%	33	5,50%	176	29,33%	
700	117	16,71%		44	6,29%	71	10,14%	34	4,86%	185	26,43%	
800	138	17,25%		45	5,63%	86	10,75%	40	5,00%	228	28,50%	
900	160	17,78%		59	6,56%	93	10,33%	42	4,67%	259	28,78%	
1000	168	16,80%		52	5,20%	99	9,90%	61	6,10%	267	26,70%	
1500	249	16,60%		102	6,80%	167	11,13%	90	6,00%	413	27,53%	
2000	329	16,45%		128	6,40%	225	11,25%	102	5,10%	567	28,35%	
2250	378	16,80%		129	5,73%	228	10,13%	118	5,24%	611	27,16%	
2500	420	16,80%		164	6,56%	263	10,52%	142	5,68%	692	27,68%	
2750	465	16,91%		169	6,15%	294	10,69%	163	5,93%	776	28,22%	
3000	523	17,43%		193	6,43%	338	11,27%	166	5,53%	871	29,03%	
10648	1814	17,04%		711	6,68%	1337	12,56%	719	6,75%	3209	30,14%	Fullfact
103823	17775	17,12%		6717	6,47%	11977	11,54%	6447	6,21%	30297	29,18%	Fullfact

Figure D.3: Samples needed for convergence, three varying parameters